NuScale Power™

LO-1217-57525

December 14, 2017

Docket: 52-048

U.S. Nuclear Regulatory Commission
ATTN: Document Control Desk
One White Flint North
11555 Rockville Pike
Rockville, MD 20852-2738

SUBJECT: NuScale Power, LLC Submittal of Technical Report "Containment Vessel Ultimate Pressure Integrity," TR-0917-56119 (NRC Docket No. 52-048)

REFERENCES: 1. NuScale Letter to the NRC, "NuScale Power, LLC Submittal of the NuScale Standard Plant Design Certification Application," dated December 31, 2016.

NuScale Power, LLC (NuScale) submitted a Design Certification Application (DCA) for its Integral Small Modular Reactor design in Reference 1. Part 2 Tier 2 of the DCA, NuScale Final Safety Analysis Report Section 3.8.2.4.5, discusses Containment Vessel (CNV) Ultimate Capacity and provides reference to the NuScale technical report "CNV Ultimate Pressure Integrity" for details of the containment internal pressure capacity.

The purpose of this letter is to provide the NuScale Technical Report "CNV Ultimate Pressure Integrity," TR-0917-56119 Revision 0. This technical report provides supplementary information, data and analyses.

Enclosure 1 contains the proprietary version of the NuScale Technical Report "CNV Ultimate Pressure Integrity," TR-0917-56119. NuScale requests that the proprietary version be withheld from public disclosure in accordance with the requirements of 10 CFR § 2.390. The enclosed affidavit (Enclosure 3) supports this request. Enclosure 1 has also been determined to contain Export Controlled Information. This information must be protected from public disclosure in accordance with the requirements of 10 CFR § 810.

Enclosure 2 contains the non-proprietary version of NuScale Technical Report "CNV Ultimate Pressure Integrity," TR-0917-56119.

This letter makes no regulatory commitments and no revisions to any existing regulatory commitments.

If you have any questions on this report, please contact Marty Bryan at 541-452-7172 or at mbryan@nuscalepower.com.

Sincerely,

Thomas A. Bergman
Vice President, Regulatory Affairs
NuScale Power, LLC

Distribution: Frank Akstulewicz, NRC, OWFN 8-H4A
Greg Cranston, NRC, OWFN-8G9A
Omid Tabatabai, NRC, OWFN-8G9A
Samuel Lee, NRC, OWFN-8G9A
Rani Franovich, NRC, OWFN-8G9A

Enclosure 1: "CNV Ultimate Pressure Integrity," TR-0917-56119-P, Revision 0, proprietary version

Enclosure 2: "CNV Ultimate Pressure Integrity," TR-0917-56119-NP, Revision 0, nonproprietary version

Enclosure 3: Affidavit of Thomas A. Bergman, AF-1217-57526

Enclosure 1:

"CNV Ultimate Pressure Integrity," TR-0917-56119-P, Revision 0, proprietary version

NuScale Power, LLC
1100 NE Circle Blvd., Suite 200 Corvallis, Oregon 97330 Office 541.360-0500 Fax 541.207.3928
www.nuscalepower.com

Enclosure 2:

"CNV Ultimate Pressure Integrity," TR-0917-56119-NP, Revision 0, nonproprietary version

NuScale Power, LLC
1100 NE Circle Blvd., Suite 200 Corvallis, Oregon 97330 Office 541.360-0500 Fax 541.207.3928
www.nuscalepower.com

Technical Report

CNV Ultimate Pressure Integrity

December 2017

Revision 0

Docket No. 52-048

NuScale Power, LLC

1100 NE Circle Blvd., Suite 200

Corvallis, Oregon 97330

www.nuscalepower.com

Technical Report

COPYRIGHT NOTICE

Department of Energy Acknowledgement and Disclaimer

This material is based upon work supported by the Department of Energy under Award Number DE-NE0000633.

Technical Report

CONTENTS

TABLES

FIGURES

Technical Report

Abstract

This report describes the methodology used to develop the containment vessel (CNV) ultimate pressure integrity for the NuScale Power LLC (NuScale) standard plant. The ultimate pressure provided in this report is the pressure the CNV can withstand before the design leakage rate of contained fluid is reached.

Calculation of the ultimate pressure follows the guidelines provided in Regulatory Guide 1.216, Revision 0 (Reference 6.1.1) and NUREG/CR-6906 (Reference 6.1.2). Material properties are based on ASME Boiler and Pressure Vessel Code, Section II material properties at design temperature.

The pressure determined within this report is for an event beyond design basis. The pressure is the lowest maximum pressure expected to cause loss of containment. The CNV ultimate pressure is less than the ASME Boiler and Pressure Vessel Code hydrostatic pressure required for Class 1 vessels. The hydrostatic pressure is based on actual testing and provides a safe pressure capacity for the fabricated vessel. The CNV ultimate pressure determination is based on conservative material behavior and provides a lowest possible ultimate pressure. Because the hydrostatic pressure and the ultimate pressure have different bases, they are not directly comparable.

Technical Report

Executive Summary

The U.S. Nuclear Regulatory Commission (NRC) regulations and guidance related to containment vessel (CNV) ultimate pressure integrity include 10 CFR 50.47, 10 CFR 50 Appendix A General Design Criterion (GDC) 50, and Regulatory Guide (RG) 1.216. Collectively these regulations and regulatory guidance require a licensee to:

I. Contain a level of design information sufficient to enable the NRC to judge the applicant's proposed means of assuring that construction conforms to the design and to reach a final conclusion on all safety questions associated with the design before the certification is granted.

II. Design the reactor containment structure, including access openings, penetrations, and the containment heat removal system so that the containment structure can accommodate, without exceeding the design leakage rate and with sufficient margin, the calculated pressure and temperature conditions resulting from any loss-of-coolant accident.

    This margin shall reflect consideration of:

    A. the effects of potential energy sources which have not been included in the determination of the peak conditions, such as energy in steam generators and energy from metal-water and other chemical reactions that may result from degradation but not total failure of emergency core cooling functioning,

    B. the limited experience and experimental data available for defining accident phenomena and containment responses, and

    C. The conservatism of the calculational model and input parameters.

III. Evaluate the pressure capacity of the CNV to determine up to what internal pressure structural integrity is retained, and a failure leading to significant release of fission products does not occur.

    This technical report specifically addresses that the details of the analysis and results should be submitted in report form with:

    A. calculated static pressure capacity;

    B. dynamic pressure capacity, if applicable (static pressure capacity reduced to account for dynamic amplification effects);

    C. associated failure modes;

    D. criteria governing the original design and criteria used to establish failure;

    E. analysis details and general results, which include

        (1) modeling details,

        (2) description of computer code(s),

(3) material properties and material modeling,

(4) loading and loading sequences,

(5) failure modes,

(6) interpretation of results, with all assumptions made in the analysis and test data (if relied upon) clearly stated and technically justified;

F. Appropriate engineering drawings adequate to allow verification of modeling and evaluation of analyses employed for the containment structure.

The CNV ultimate pressure integrity is calculated using multiple, non-linear, finite-element analyses to evaluate failure criteria established for bolted connections, shell regions away from concentrations, and buckling in the top and bottom heads. This report presents the methodology used to determine the CNV ultimate pressure integrity and the value of the CNV ultimate pressure for the NuScale standard containment vessel. The ultimate pressure is calculated based on the methodology provided in Regulatory Guide 1.216. The calculated pressure is below the physical hydrostatic test pressure required by Section III of the ASME Boiler and Pressure Vessel Code for Class 1 vessels. The ultimate and hydrostatic pressure values are determined by different bases and are therefore not comparable.

Technical Report

1.0 Introduction

1.1 Purpose

This report describes the methodology, ultimate pressure, and method of failure for the NuScale Power, LLC (NuScale) containment vessel (CNV) internal pressure capacity for a beyond design basis loss-of-coolant accident (LOCA). This report and methodology is in accordance with Standard Review Plan Section 3.8.2 (Reference 6.1.3) and Nuclear Regulatory Commission (NRC) Regulatory Guide (RG) 1.216 (Reference 6.1.1).

1.2 Scope

This report provides the methodology for developing the CNV ultimate pressure integrity for the NuScale standard plant CNV. The 10 CFR 50, Appendix A, General Design Criterion 50, “Containment Design Basis,” requires that “the reactor containment structure and its internal components can accommodate, without exceeding the design leakage rate and with sufficient margin, the calculated pressure and temperature conditions caused by a LOCA.”

This report discusses the non-linear (plastic), three-dimensional (3-D), finite element analyses that conform to the guidelines in NUREG/CR-6906 (Reference 6.1.2). The report addresses all CNV penetrations and includes the evaluation of buckling in the CNV heads. This report addresses the following six aspects:

- design internal pressure,
- static pressure capacity,
- dynamic pressure capacity,
- failure modes,
- criteria used to establish failures, and
- analysis details, including (1) modeling details; (2) material properties; (3) loading and loading sequence; (4) computer codes used; (5) failure modes; and (6) interpretation of results.

This report does not provide the ultimate pressure capacity for as-built plants. These limits may be created on a unit-specific basis with consideration of as-built material properties and as-built CNV dimensions. The as-built evaluation may reference the methods used in this report to develop the unit-specific ultimate pressure capacity. The combustible gas inside containment is addressed in TR-0716-50424 and is not within the scope of this report.

1.3 Abbreviations and Definitions

The abbreviations used in this report are shown in Table 1-1. Definitions of common terms used in the report are shown in Table 1-2.

Table 1-1 Abbreviations

Term	Definition
ASME	American Society of Mechanical Engineers
BPVC	Boiler and Pressure Vessel Code
CNV	containment vessel
CRDM	control rod drive mechanism
FEA	finite element analysis
GDC	General Design Criteria
ID	inside diameter
LOCA	loss of coolant accident
LWR	light water reactor
NPS	Nominal Pipe Size
NRC	Nuclear Regulatory Commission
OD	outside diameter
RCS	reactor coolant system
RG	Regulatory Guide
RPV	reactor pressure vessel
SG	steam generator
SSC	systems, structures and components

Table 1-2 Definitions

Term	Definition
Bolt	Bolt and stud are used interchangeably for a headless, threaded rod fastener.
CNV refueling flanges	Set of large-diameter flanges located on the CNV that are unbolted during a refueling outage to provide access to the reactor pressure vessel (RPV).
Preload	The tension created in a fastener when it is tightened.
O-ring	A gasket in the form of a ring (typically with a circular cross section) used to seal bolted flange connections.

2.0 Background

The NuScale Power Module design differs from other light water reactor designs currently in operation in that the CNV is designed, fabricated, inspected, tested, and stamped as an American Society of Mechanical Engineers (ASME) Boiler and Pressure Vessel Code (BPVC) Class 1 pressure vessel. The design pressure for the NuScale CNV is approximately one order of magnitude higher than other light water reactor designs currently in operation. The NuScale Power CNV is partially immersed in the reactor pool to facilitate heat removal. The CNV is designed to provide a barrier against the release of fission products while accommodating the calculated pressures and temperatures resulting from postulated mass and energy release inside containment. The CNV is designed to withstand the full spectrum of postulated mass and energy releases (i.e. LOCA and non-LOCA, including combustible gas events.)

This report discusses the methodology and modes of failure for a beyond design basis LOCA event that creates an increasing internal pressure. It determines at what pressure containment integrity is lost.

Dynamic pressure as a result of hydrogen detonation is not evaluated in this report. The NuScale CNV structural integrity analysis of design basis and beyond design basis hydrogen combustion events are discussed in TR-0716-50424.

2.1 Regulatory Requirements

2.1.1 10 CFR 50 Appendix A GDC 50 and 10 CFR 50.44

In accordance with General Design Criterion (GDC) 50 and 10 CFR 50.44, the reactor containment structure, including access openings, penetrations, and the containment heat removal system shall be designed so that the containment structure and its internal compartments can accommodate, without exceeding the design leakage rate and with sufficient margin, the calculated pressure and temperature conditions resulting from any LOCA.

This margin shall reflect consideration of (1) the effects of potential energy sources that have not been included in the determination of the peak conditions, such as energy in steam generators (SGs) and as required by 10 CFR 50.44 energy from metal-water and other chemical reactions that may result from degradation but not total failure of emergency core cooling functioning, (2) the limited experience and experimental data available for defining accident phenomena and containment responses, and (3) the conservatism of the calculational model and input parameters.

2.1.2 10 CFR 52.47

The application must contain a level of design information sufficient to enable the Commission to judge the applicant's proposed means of assuring that construction conforms to the design and to reach a final conclusion on all safety questions associated with the design before the certification is granted. The information submitted for a design certification must include performance requirements and design information sufficiently detailed to permit the preparation of acceptance and inspection requirements by the NRC, and procurement specifications and construction and installation specifications by an applicant.

2.1.3 Regulation Guide 1.216 - Containment Structural Integrity Evaluation for Internal Pressure Loading above Design Basis Pressure

RG 1.216 provides guidance for the methods to (1) predict the internal pressure capacity for containment above design basis accident pressure, (2) demonstrate containment structural integrity related to combustible gas control, and (3) demonstrate containment structural integrity for Class MC steel containment through an analysis to prevent and mitigate severe accidents. The basis of RG 1.216 does not include considerations for containment vessels designed and fabricated in accordance with ASME Class 1 requirements.

Specifically this report addresses RG 1.216, Section C.1.k which states that the details of the analysis and results should be submitted in report form with:

- calculated static pressure capacity;
- dynamic pressure capacity, if applicable (static pressure capacity reduced to account for dynamic amplification effects);
- associated failure modes;
- criteria governing the original design and criteria used to establish failure;
- analysis details and general results, which include (1) modeling details, (2) description of computer code(s), (3) material properties and material modeling, (4) loading and loading sequences, (5) failure modes, and (6) interpretation of results, with all assumptions made in the analysis and test data (if relied upon) clearly stated and technically justified; and,
- appropriate engineering drawings adequate to allow verification of modeling and evaluation of analyses employed for the containment structure.

2.1.4 NUREG/CR-6906 – Containment Integrity Research at Sandia National Laboratories

NUREG/CR-6906 is a report summarizing research performed at Sandia National Labs for nearly thirty years on nuclear power plant steel containment structures and their response to extreme loads beyond their design basis. Containments considered in this Sandia National Lab report included large pressure water reactor and boiling water

reactor steel as well as concrete-reinforced containment designs. No containments designed and fabricated to ASME Boiler and Pressure Vessel Code, Section III Class 1 requirements were considered.The report summarizes the work that has been performed and the results of the efforts, and identifies common themes that have emerged. Appendix A provides guidelines for containment capacity analysis to evaluate containment structures subject to beyond design basis accident loads.

3.0 Analysis of Containment for Ultimate Pressure Integrity

3.1 Failure Criteria for CNV Ultimate Pressure Capacity

The failure criteria guidelines that determine the ultimate pressure capacity of the CNV are provided in Reference 6.1.1, Section C.1. The NuScale CNV is assumed to fail when one of the following criteria is met:

A. A maximum flange gap of 0.03 inches between the flange cover and top of flange at the center of the outer O-ring is reached at any CNV bolted opening. The maximum gap is estimated based on a review of O-ring groove depth tolerances of several O-ring manufacturer catalogs;

B. Loss of bolt preload occurs at any bolted CNV opening;

C. A maximum global membrane strain away from discontinuities of 1.5 percent is reached;

D. Solution divergence occurs;

E. Buckling occurs at the knuckle of the top or bottom CNV head.

For failure criterion C, the maximum global membrane strain (hoop membrane strain) away from discontinuities (i.e., openings, changes in diameter, etc.) is defined as the maximum hoop strain calculated through the CNV wall at a distance of $2.5\sqrt{(Rt)}$ from the discontinuity, where “R” is the inside radius of the CNV and “t” is the wall thickness at the location of the discontinuity.

Note that Reference 6.1.1 states that the potential for containment leakage at pressure levels below the calculated pressure capacity also should be considered by comparing the total calculated leakage against a defined total leakage limit. Because at the time the CNV ultimate pressure integrity was calculated a leakage limit (or leakage acceptance criterion) had not been established, failure criterion A conservatively assumes that an unacceptable leakage is reached when a small gap forms at the outer O-ring. Flange leakage is negligible at or below the small flange gap of failure criterion A.

3.2 Methodology

A non-linear, static, structural 3-D finite element analysis (FEA) is performed using multilinear kinematic hardening material properties to determine the ultimate pressure capacity of the CNV. Small strain is assumed for all FEA models (i.e., the large deflection option is turned off). The 3-D geometry for all models is imported into ANSYS® Workbench™ prior to splitting the CNV into separate models, as described in Section 3.4 and simplifying, as described in Section 3.4.1.

3.3 Geometry and Material Inputs

The following geometry and material inputs are used in this report.

3.3.1 Geometry

The geometry used in this calculation is based on the 3-D solid model of the CNV assembly, and drawings of the following subassemblies:

- CNV top head assembly
- CNV upper section
- Lower CNV section
- Electrical penetration assembly

Cladding is included and credited.

3.3.2 Materials

The materials for the components in this report are shown in Table 3-1.

Table 3-1 Materials

Component[1]	Material
CNV Top Head Cover Control Rod Drive Mechanism (CRDM) Access Opening	SA-182, Type F304 (thickness > 5 in)
CNV Top Head	SA-508, Grade 3, Class 2
CNV Upper Section – all shells above refueling flanges	SA-508, Grade 3, Class 2
CNV Lower Section – all shells below refueling flanges (except CNV support skirt)	SA-965, FXM-19
Cladding[2]	Type 308L & 309L stainless steel
Fasteners (studs, nuts, washers) used for CNV Top Head bolted openings	SA-564, Grade 630 (17-4 PH), Condition H1100
Fasteners (studs, nuts, washers) used for CNV Upper Section bolted openings	SB-637 Alloy N07718
Flange Covers	SA-240, Type 304
Threaded Inserts	SA-479, Type 316

Notes:
1. The CNV is constructed of multiple shell sections welded together. Weld material and properties are not considered in this calculation. The mechanical properties of the CNV Class 1 welds are at least equal to the properties of the parent material. (CNV Class 1 full-penetration welds are shop-fabricated and post-weld heat treated.) Failure of the CNV will not occur at the welds or in the heat-affected zone of the parent material as a result of reduced material properties. The CNV Class 1 welds are post-weld heat treated prior to going into service to minimize residual stresses at the welds.
2. Outside surfaces of the CNV low-alloy shells/forgings are clad with austenitic stainless steel. The cladding is deposited in two passes of Type 309L and Type 308L stainless steels. Inside surfaces of the CNV low-alloy steel shells/forgings are clad with one pass of 309L austenitic stainless steel.

3.3.3 Material Properties

The material properties used in this report, for the components identified in Section 3.3.2, are provided in Reference 6.1.6. Material properties are defined at the CNV design temperature. The material properties for SA-240, Type 304L are applied to the cladding materials. The cladding material properties (SA-240, Type 304L) are applied

to the threaded inserts (SA-479, Type 316). Materials are defined as multilinear kinematic hardening with the slope of the true stress-true strain line between yield strength and ultimate tensile strength determined by the uniform elongation of the material.

The guidance of Reference 6.1.1, Section C.1.d specifies that the non-linear stress-strain curve be based on the ASME BPVC minimum yield strength, and the stress-strain beyond yield representative of the specific grade. Appendix B shows a comparison of the material non-linear curve used in the analysis to the material's true stress–true strain curve using the ASME BPVC minimum properties at design temperature. The comparisons show that the material non-linear curves used in the analysis are conservative and provide a reasonable representation of the material behavior in the strain region being evaluated.

Reference 6.1.1, Section C.1.d specifies that the stress–strain curve used in the analysis corresponds to the design basis accident temperature. Conservatively, the stress-strain curve used in this report is based on design temperature. See Section 3.5.7 for a discussion of how design temperature relates to a conservative beyond design basis event temperature.

Material properties shown in Table 3-2 are taken from Reference 6.1.6. Since weld (including weld deposited cladding) metals are typically stronger than their base metal counterparts, the mechanical and thermal properties of the base metal are used for the welds. Multilinear kinematic hardening properties are used for plastic FEA.

Table 3-2 Material properties at design temperature (550 degrees Fahrenheit)

Material	Poisson's Ratio (unit less)	Modulus of Elasticity ($x10^6$ psi)	Yield Strength (psi)	Ultimate Tensile Strength (psi)	Elongation(1) (%)
SA-182, Grade F304 (thickness > 5 in)	0.3	25.6	18,900	59,200	30
SA-508, Grade 3, Class 2	0.3	25.4	55,400	90,000	16
SA-965, FXM-19	0.3	25.6	38,100	88,400	30
SA-240, Type 304	0.3	25.6	18,900	63,400	40
SA-240, Type 304L	0.3	25.6	16,000	57,200	40
SB-637 Alloy N07718(2)	0.29	27.0	136,100	167,800	12
SA-564, Grade 630 (17-4 PH), Condition H1100	0.3	25.8	94,000	132,400	14

Notes:
1. Uniform elongation at room temperature tensile failure.
2. SB-637 Alloy N07718 yield strength is calculated as $3S_m$ and ultimate tensile strength is extrapolated based on the ratio of yield strength to ultimate strength at room temperature.

3.4 Finite Element Analysis Model Summary

Due to the complexity and computational cost of creating a single global ANSYS® model of the CNV, five models were created as summarized below and illustrated in Figure 3-1. The five models are put into two groups for discussion purposes. One group is the CNV pressure capacity models and the second group is the CNV head buckling models. The first three models are the CNV pressure capacity models. These models are used to establish the internal pressure capacity of the CNV. The models are sectioned as described below by exploiting symmetry about the CNV centerline. The remaining two models are the CNV head buckling models. The CNV head buckling models are used to estimate the internal pressure needed to produce buckling in the CNV head knuckles (see Section 3.6). As specified in Reference 6.1.1, Section C.1.a, use of a half or wedge 3-D finite element model is acceptable to use.

CNV Pressure Capacity Models:

1. CNV Top Section Model

    - A quarter segment (0 to 90-degree segment) of the total CNV top section was modeled. One slice plane is through the top head centerline along the 90 to 270-degree axis passing through[1]: the CNV Head Manway 18 in. diameter (CNV24); the CRDM Access Opening – 67 in. diameter (CNV25); and the CRDM Power Opening – 18 in. diameter (CNV37). The second slice is through the 0 to 180-degree plane. The blue segment shown in Figure 3-2 shows the segment modeled and actual alignment of openings. The yellow highlighted openings show the penetrations adjusted to align on the cut plane axis.
    - Nozzle penetrations and instrumentation and control openings less than nominal pipe size (NPS) 18 were not modeled.
    - Parent material, cladding and threaded inserts were modeled as separate material properties with shared boundaries. Other bolting components were modeled as separate parts.
    - Fasteners were modeled using minimum minor (thread root) bolt diameters.

2. CNV Middle Section Model

    - A one-eighth slice of the total CNV middle section was modeled. One slice plane is through the centerlines of the SG inspection port (CNV30) and the second plane is through the pressurizer heater access port (CNV31). The blue segment shown in Figure 3-3 shows the segment modeled and actual alignment of openings.

      After the analysis of the CNV ultimate pressure was performed the design was modified to add 7.5 inches of reinforcement around the pressurizer access port opening on the inside surface of the CNV. The additional reinforcement is shown in Figure 3-3 below, but is not included in the CNV Ultimate Pressure Capacity middle section model. The added reinforcement serves to stiffen the CNV shell around the opening and produce less distortion of the access flange. This additional reinforcement produces a smaller and more uniform deflection of the flange. More deflection of the cover due to a higher pressure is therefore needed to reach the failure criteria specified in Section 3.1. Therefore, the resultant calculated CNV ultimate

[1] Note: The CNV head manway and CRDM power opening (highlighted in yellow in Figure 3-2) are rotated about the CNV centerline such that they align with the 90-degree axis of the top head. The slight geometric discretization does not impact the results.

pressure produces a lower, bounding ultimate pressure from that expected with the added reinforcement.

- The model segment includes the RPV support on the CNV inside surface. The CNV middle section model was used to evaluate membrane strain due to pressure away from local effects per the guidance of Reference 6.1.1, Section C.1.f.4. The RPV support analyzed applies a load and moment to the wall that reasonably represents the support design.

  The RPV support design has been revised slightly from that modeled in this analysis. The support is 2.532 inches below the analyzed support location. The attachment bolt is also moved away from the CNV wall by an additional 4.325 inches. Since this model is used only to evaluate membrane strain due to pressure away from local effects per the guidance of RG 1.216 Section C.1.f.4, the revised RPV support does not affect the CNV Ultimate Pressure Capacity results.

- Parent material, cladding and threaded inserts were modeled as separate material properties with shared boundaries. Other bolting components were modeled as separate parts.

- Fasteners were modeled using minimum minor (thread root) bolt diameters.

3. CNV Bottom Section Model

   - A 1/96 slice of the total CNV bottom section was modeled. The model includes the refueling flanges and a closure bolt. One slice plane is through the centerline of the CNV and passes through the centerline of the closure bolt on the 0-degree axis. The second slice plane passes mid-way between closure studs. The blue segment in Figure 3-4 shows the segment modeled and alignment with the closure studs.

   - Parent material and cladding were modeled as separate material properties with shared boundaries. Other bolting components were modeled as separate parts.

   - Fasteners were modeled using minimum minor (thread root) bolt diameters.

CNV Head Buckling Models:

4. Top Head Buckling Model

   - A full 360-degree CNV top head is modeled. The model includes the CNV Head Manway 18 in. diameter (CNV24) and the CRDM Access opening – 67 in. diameter (CNV25) openings, without covers.

   - Nozzle penetrations and small instrumentation and control openings less than NPS 18 were not modeled.

- Parent material and cladding were modeled as separate material properties with shared boundaries.
- Fasteners, including threaded inserts were not included.

5. Bottom Head Buckling Model
    - A full, 360-degree CNV bottom head was modeled. There are no penetrations in the CNV bottom head. The CNV support skirt on the outside of the bottom head was included in the model.
    - The design of the reactor pressure vessel (RPV) lateral support located on the dome of the bottom head has subsequently been revised. The pin and retainer modeled in the analysis had the pin located on the bottom, inside surface of the CNV, and the retainer on the bottom, outside surface of the RPV. After completion of the analysis the design was modified to the current design with the pin located on the RPV and the retainer on the CNV. Since the RPV lateral support is located at the center of the dome and remote from the knuckle, it provides no additional support to the knuckle. Therefore, this design change has no impact on the buckling of the knuckle due to internal pressure.

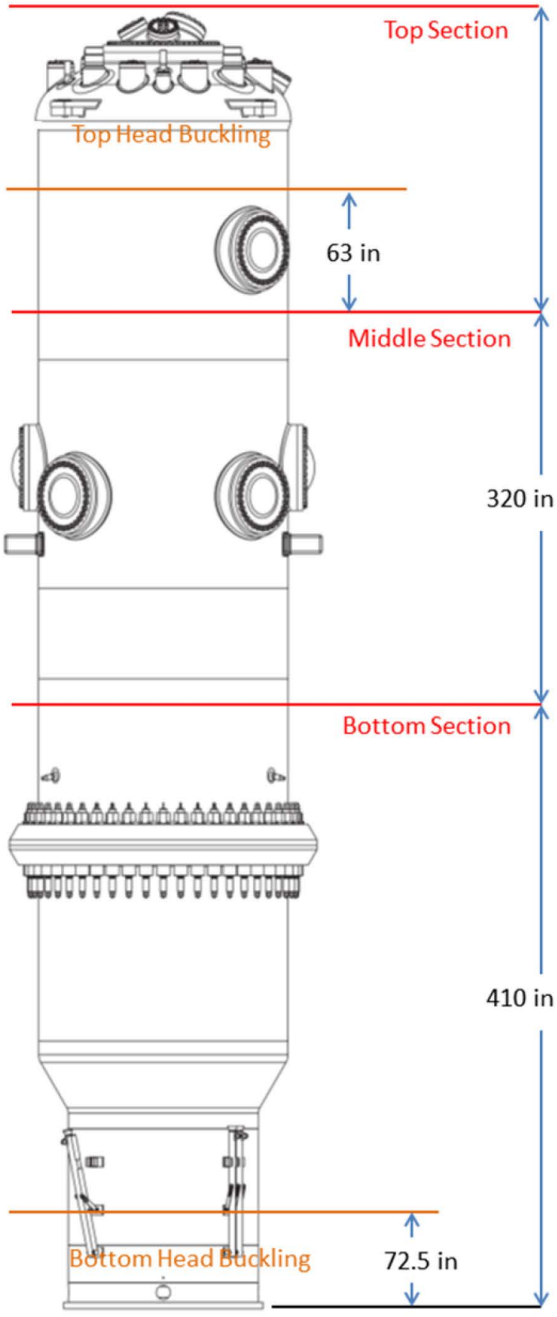

Figure 3-1 CNV sectioning (slice planes) for finite element analysis modeling

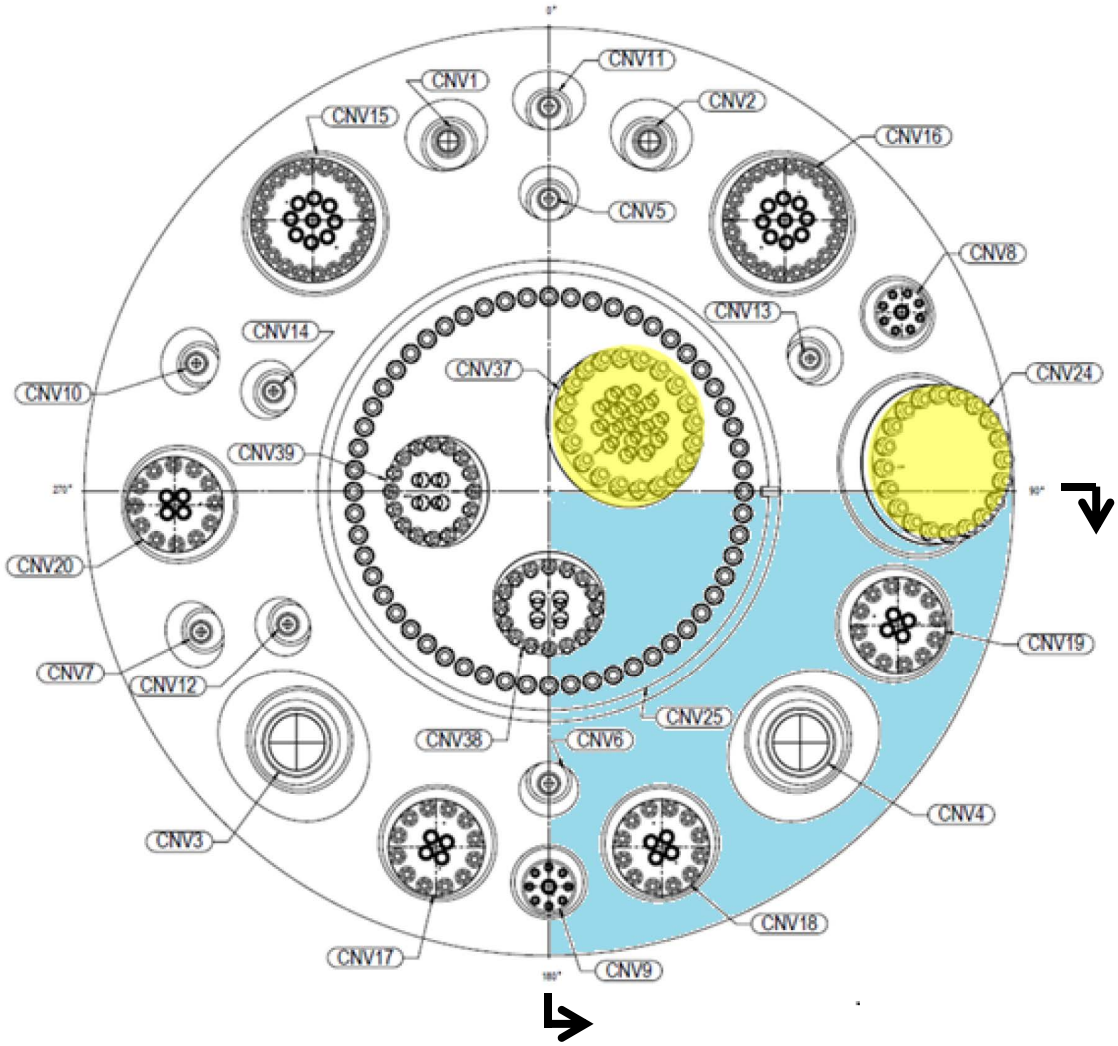

Figure 3-2 CNV top section model alignment (NOTE: platform mounts not shown)

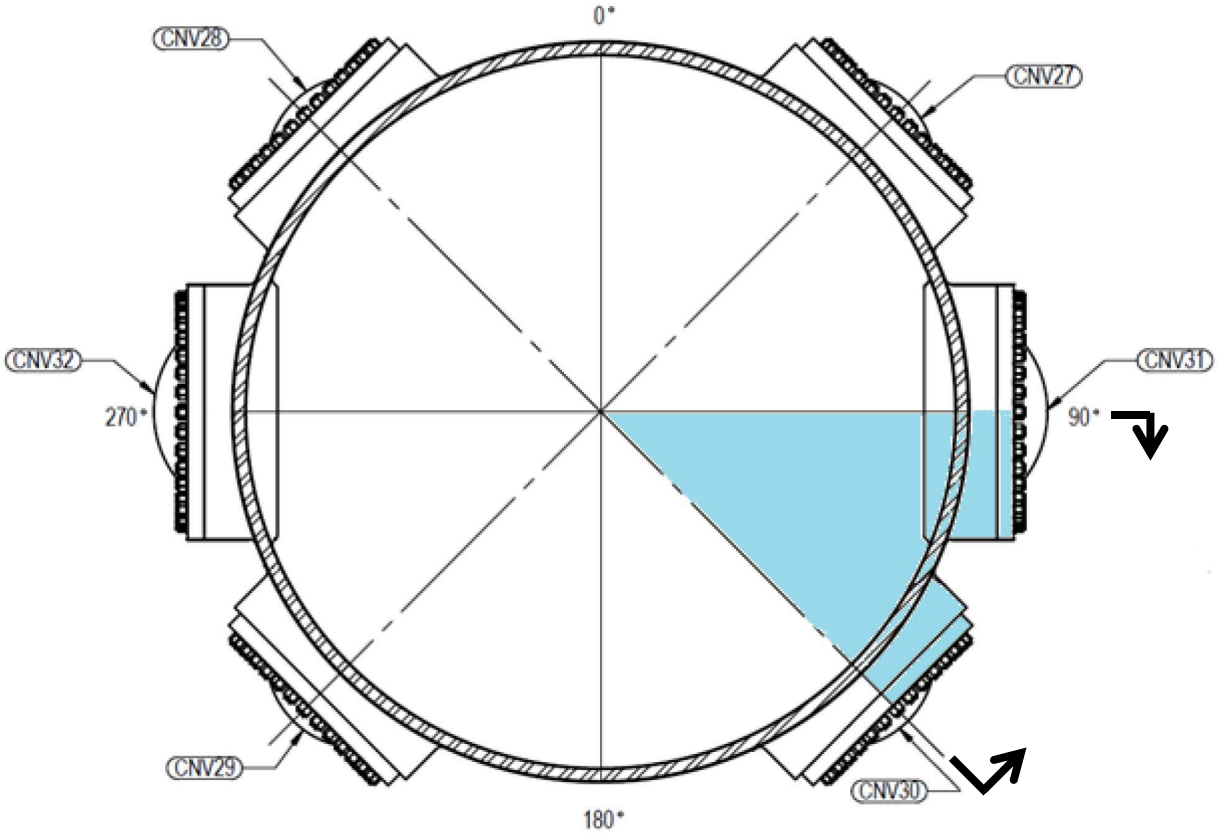

Figure 3-3 CNV middle section model alignment

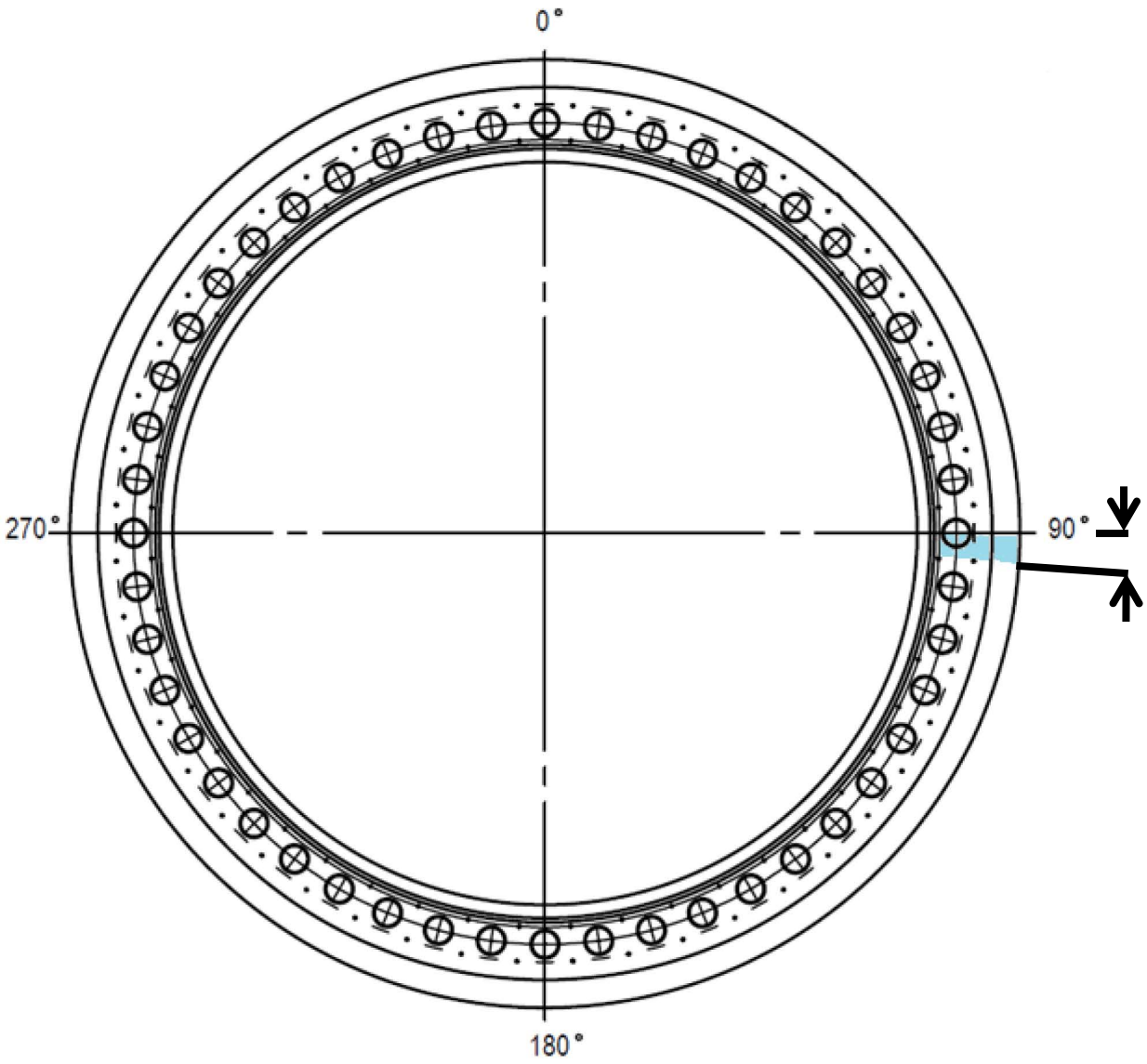

Figure 3-4 CNV bottom section model alignment

3.4.1 Modeling Simplification

Per the guidance in Reference 6.1.2, Appendix A, small CNV penetrations can be reasonably ignored in terms of their effect on the overall containment response. The proximity of these penetrations to CNV bolted openings does not negatively impact the ultimate pressure capacity of the CNV.

The electrical penetrations, top support structure support with frame, and piping penetrations (i.e., feedwater lines, steam lines, containment isolation valves, etc.) do not impact the ultimate pressure capacity of the CNV and are excluded from FEA models. In addition, the bolted openings with an inner nozzle diameter smaller than NPS 18 do not limit the ultimate pressure capacity of the CNV and are not modeled. Since the force on a bolted flange cover is proportional to the square of the diameter on which the pressure acts, the larger-diameter bolted openings fail before smaller-diameter bolted openings.

The following general modeling simplifications are also made to the 3-D solid model before sectioning the CNV to create the ANSYS® models identified in Section 3.4:

- Remove chamfers, small radius fillets, alignment features
- Remove O-ring grooves
- Remove CNV nozzle penetrations
- Remove bolted openings smaller than NPS 18
- Remove top support structure frame and supports
- Remove vent holes from support skirt
- Remove components external to the CNV shell (support lugs, lifting trunnions, etc.)
- The welds are full-penetration welds and modeled as part of the base metal and are not modeled as a separate, integral part. The mechanical properties of the CNV Class 1 welds (Note: CNV Class 1 welds are full-penetration, shop-fabricated welds) are at least equal to the properties of the parent material and failure of the CNV does not occur at the welds or in the heat-affected zone of the parent material as a result of reduced material properties. The CNV Class 1 welds are post-weld, heat treated, and fully inspected prior to going into service to minimize residual stresses at the welds

The modeling features described above do not affect the overall structural behavior of the models, but allow for simplified meshing and reduced element counts. This is standard industry practice for perfoming finite element analysis.

3.4.2 Coordinate Systems

For each of the models described in Section 3.4, a Cartesian global coordinate system is used. The origin of the models is at the intersection of the CNV centerline with the reactor pool floor (NuScale Power Module global zero). Models have the positive Y-axis as the vertical axis with the positive X-axis in the 90-degree direction and, following the right-hand rule,the positive Z-axis in the 180-degree direction.

3.4.3 Contact Regions

Frictional contacts, which allow separation and produce a frictional force when sliding occurs, are applied to the following connections on the ANSYS® models:

- Bottom of nuts to top of washers on flange covers[2]
- Bottom of washers to top of flange covers
- Bottom of bolted flange covers to the top of flange
- A coefficient of friction of 0.2 is applied to the frictional contacts. The coefficient of friction for wet steel is applicable to the CNV bolted openings because the CNV operates in a submerged/wet environment. The coefficient of friction of wet steel is taken to be equal to that of greased steel, based on the value in Reference 6.1.11. A lower coefficient of friction results in conservative flange gap values.

Bonded contacts, which allow no separation or sliding are applied to the following connections:

- Outer diameter (OD) of studs to inner diameter (ID) of nuts and to threaded inserts/bolt holes

There is a diametrical clearance between studs passing through the flange covers and the studs passing through the CNV refueling flanges. No contact is therefore applied at these surfaces.

3.5 CNV Pressure Capacity Analysis

The following sections discuss the boundary conditions and load application for the three CNV pressure capacity ANSYS® models. CNV head buckling model boundary conditions and loads are discussed in Section 3.6.

[2] In the CNV bottom section model, the washer is combined with the top nut, forming a single part. Therefore, a contact region between the nut and washer is not defined.

3.5.1 CNV Pressure Capacity - Symmetry Plane

The three CNV pressure capacity models apply a symmetry boundary condition (constraint of the displacement normal to the plane) to the vertical plane slicing the global X-Y plane of the model. Applied loads to the three models are symmetric about the global X-Y plane. The symmetry boundary condition applied to the ANSYS® models is shown as a red surface in Figure 3-5.

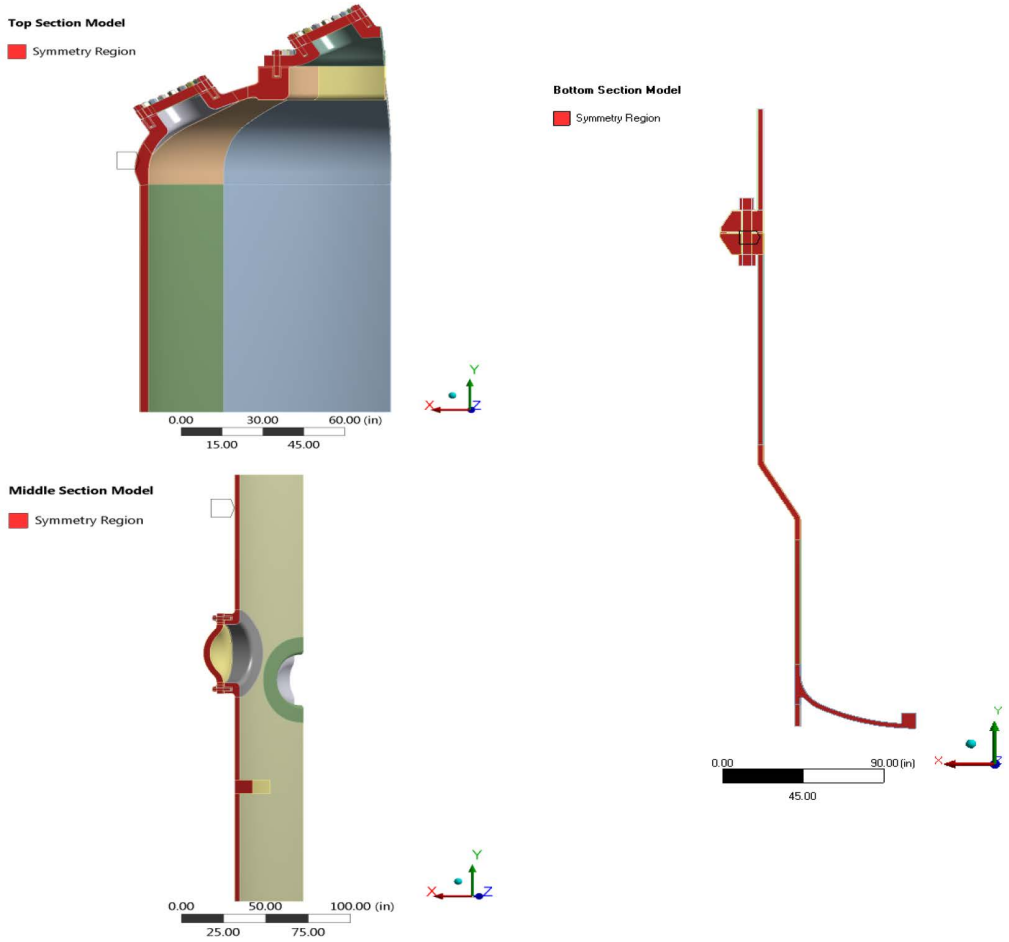

Figure 3-5 Symmetry boundary condition (clockwise from top left: CNV top section model, CNV bottom section model, CNV middle section model)

3.5.2 CNV Pressure Capacity - Frictionless Supports

For each of the ANSYS® models forming the CNV shell, two frictionless support boundary conditions are applied. The frictionless support constrains the displacement normal to the plane and allows the plane to freely move in the transverse direction.

One frictionless support is applied to a horizontal plane perpendicular to the CNV centerline. This support prevents rigid body motion in the vertical (parallel to the Y-axis) direction. No additional vertical support is applied to allow each model to grow vertically (parallel to the Y-axis). The second frictionless support boundary condition is applied at the other vertical face (parallel to the Y-axis) created by the slice plane through the CNV centerline at an angle from the global X-Y plane. This support simulates the restraining effects of the material on the other side of the slice plane.

The frictionless support boundary conditions applied to the CNV pressure capacity ANSYS® models are shown as a blue surface Figure 3-6.

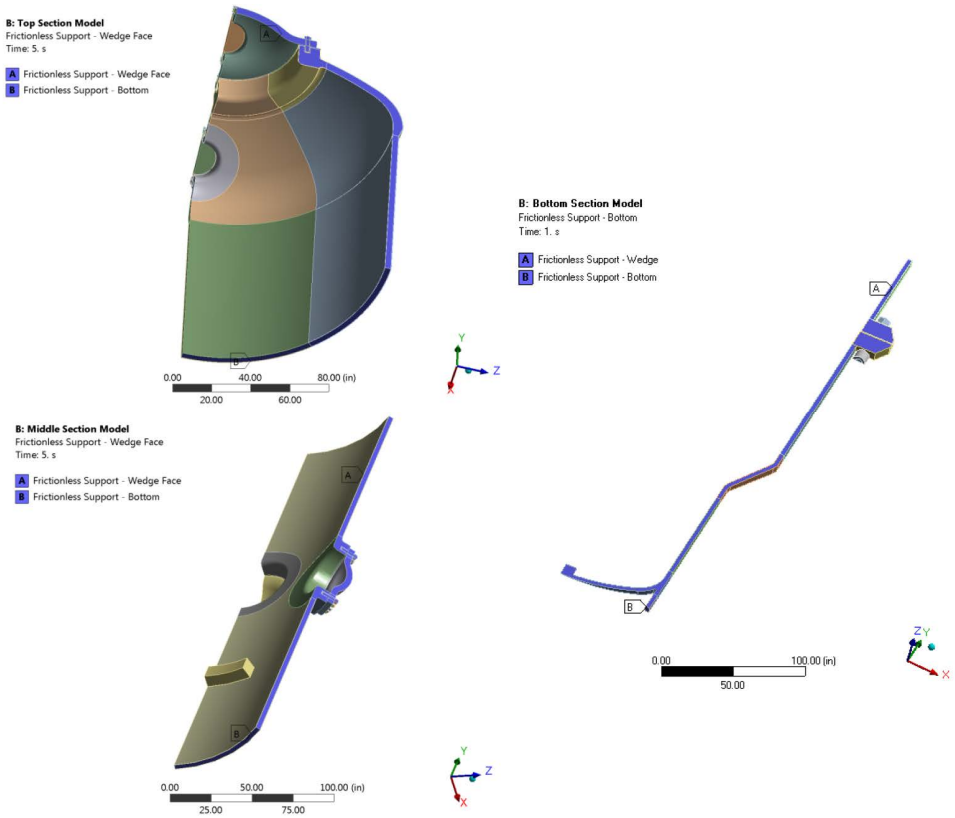

Figure 3-6 Frictionless support (clockwise from top left: CNV top section model, CNV bottom section model, CNV middle section model)

3.5.3 CNV Pressure Capacity - Gravity, Dead Weight and Buoyancy Loads

The total weight of the RPV and reactor coolant system water used in the analysis is {{ }}$^{2(a)(c), ECI}$. The water weight includes water in the CNV and RPV at the time the module is assembled. During a LOCA event the only water in the CNV is what exists inside of the RPV. So the total weight conservatively includes not only a 3 percent contingency, but also additional water weight. The components and their individual weights are shown in Table 3-3.

The weight of the water considered in the CNV is about {{ }}$^{2(a)(c), ECI}$ of the total water weight. So when this is subtracted from the total RPV weight, the RPV weight during operation is {{ }}$^{2(a)(c), ECI}$, which is less than the weight evaluated.

The CNV is partially immersed in the reactor pool during operation up to approximately the bottom of the top head. The reactor pool provides a buoyancy load, reducing the dead weight load carried by the CNV support. The reduction in load created by buoyancy is not included and the full dead-weight load is used in the analyses.

A standard earth gravity load is applied to the bodies in the CNV pressure capacity ANSYS® models forming the CNV shell. The gravity load acts in the -Y direction at the center of gravity determined by ANSYS® Mechanical™.

In addition to the gravity load, a dead weight load equal to one-eighth of the weight of the RPV and reactor coolant system water (one-eighth of {{ }}$^{2(a)(c), ECI}$ as discussed above) is applied in the CNV middle section model to the RPV support lug, acting in the -Y direction. This load is applied as a force of {{ }}$^{2(a)(c), ECI}$ acting on the RPV support section in the model. Conservatively, this dead load is not applied to the CNV bottom section model because it would act to reduce the force prying open the CNV refueling flanges.

The dead weight of the top support structure, including instrumentation (about {{ }}$^{2(a)(c), ECI}$) does not impact the ultimate pressure capacity of the CNV and is excluded. The weight of the top support structure is transferred to the CNV through four platform mount supports on the CNV top head, mainly resulting in shear loads on four areas on the outside surface of the CNV top head. These loads are small relative to the hoop stress induced in the CNV due to internal pressure. Therefore, loads due to the top support structure are not included in the dead weight loads.

Table 3-3 RPV component weight

Component	Weight[(1)(3)]	Units
RPV	{{ }}[2(a)(c), ECI]	lbf
Water[(2)]	{{ }}[2(a)(c), ECI]	lbf
Reactor vessel internals	{{ }}[2(a)(c), ECI]	lbf
SG	{{ }}[2(a)(c), ECI]	lbf
CRDM	{{ }}[2(a)(c), ECI]	lbf
Control rod assembly	688	lbf
Fuel	30,710	lbf
Valves	{{ }}[2(a)(c), ECI]	lbf
Total[(3)]	{{ }}[2(a)(c), ECI]	lbf
CNV water weight[(4)]	{{ }}[2(a)(c), ECI]	lbf
Total weight during operation	{{ }}[2(a)(c), ECI]	lbf

Notes:

1. Includes 3 percent contingency to cover tolerance variation and components not included
2. Contingency not on water. Weight includes water in the CNV and RPV up to the baffle plate. Water weight is based on water density at 100 degrees Fahrenheit.
3. Components not included:
   - Neutron source assemblies
   - O-rings
   - CRDM cooling water and water hoses
   - small lines
   - integral shield restraints
   - electrical penetration assemblies
4. Approximate water weight in CNV.

3.5.4 CNV Pressure Capacity - Internal Pressure

Two internal pressures load steps are applied to the inside CNV surfaces of each ANSYS® model (see Section 3.5.8). The first pressure applied is the initial pressure at the CNV design pressure of 1,000 psi and the second pressure is at {{ }}[2(a)(c), ECI]. For bolted openings, the pressure is applied to the surface bounded by the outer O-ring groove of the flange cover.

Since the endcap pressure, as discussed in Section 3.5.5, is directly proportional to the internal pressure, the endcap pressure is also applied in two load steps.

The 1,000 psi internal pressure load applied to the CNV pressure capacity ANSYS® models is shown by the red surface in Figure 3-7.

{{

}}2(a),(c),ECI

Figure 3-7 Internal pressure load (clockwise from top left: CNV top section model, CNV bottom section model, CNV middle section model)

3.5.5 CNV Pressure Capacity - Endcap Pressure Load

Due to the closed ends of the CNV (endcaps), a load is induced in the CNV shell when the CNV is pressurized. This total endcap pressure is calculated as follows:

$$P_{endcap} = -\frac{D_i^2 P_{internal}}{D_o^2 - D_i^2}$$ Equation 3-1

Where:

D_i = the inner diameter (ID) of the main CNV shell (including cladding)

$P_{internal}$ = the internal pressure of the CNV

D_o = the OD of the main CNV shell (including cladding)

For static equilibrium, this endcap pressure is only applied to the CNV middle section and CNV bottom section models as a vertical (parallel to the Y-axis) pressure load acting outward. The red surface in Figure 3-8 shows where the pressure load is applied. The CNV top section model has the top head surface modeled. When the internal pressure is applied, and with the bottom of the model constrained vertically, the endcap load is accounted for in the model.

{{

}}2(a),(c),ECI

Figure 3-8 CNV middle section model (left) and CNV bottom section model (right) endcap pressure

3.5.6 CNV Pressure Capacity - Stud Preload

Gaskets used to seal the CNV bolted openings are of the self-energizing O-ring type or similar. Therefore, for the flanged openings on the CNV, zero compression pressure is required to produce a seal. Per Reference 6.1.8, Table E-1210-1, the gasket factor, m, and minimum design seating stress, y, are both zero.

The individual stud preload for the CNV refueling flange is {{ }}[2(a)(c), ECI] The stud preload for other fasteners is calculated based on two-thirds of the yield strength (i.e., two times the design stress intensity) of the studs at design temperature. The stud preload is applied at cold conditions through direct tension. Thermal stress relaxation effects are not considered. Two times the design stress intensity is the maximum allowable stress, averaged across the bolt cross section, per Reference 6.1.7, subparagraph NB-3232.1:

A maximum stud preload (per stud) is calculated using the following equation:

$$F_{preload} = \frac{2S_y}{3} \cdot \frac{\pi D_r^2}{4} = \frac{S_y \pi D_r^2}{6}$$ Equation 3-2

Where:

S_y = the yield strength at the design temperature

D_r = the minimum minor (thread root) diameter of the stud. See Appendix C for the stud preload and minimum minor diameter calculations.

The stud minimum minor diameter, D_r, is calculated for the external threads per Reference 6.1.10, Paragraph 8.3.1(f):

$$D_r = D_{P\_min} - 0.64951905(P_{thread})$$ Equation 3-3

Where:

D_{P_min} = the minimum pitch diameter of external thread

P_{thread} = the thread pitch.

Stud preloads are applied to the modeled studs using the bolt pretension load type in two load steps. The preload is applied in the first load step and locked in the second load step. The stud preload is applied at a temperature of 70 degrees Fahrenheit.

Figure 3-9 shows the stud preload after it is locked for bolted openings: CNV top head manway (CNV24), CRDM access (CNV25), CRDM electrical (CNV37), SG Inspection (CNV30), PZR heater (CNV31) and the CNV refueling flanges.

{{

}}2(a),(c),ECI

Figure 3-9 Stud preload (clockwise from top left: CNV top section model, CNV middle section model, CNV bottom section model)

3.5.7 CNV Pressure Capacity - Thermal Condition

For the CNV pressure capacity ANSYS® models, two uniform thermal conditions are applied to the bodies. An initial uniform metal temperature of 70 degrees Fahrenheit is applied to the CNV for bolt tensioning. The second thermal condition is the CNV design temperature of 550 degrees Fahrenheit applied for both internal pressure loads. The guidance provided in Reference 6.1.1, Section C.1.d specifies that the analysis correspond to the design basis accident temperature. Justification is provided below that use of the design temperature is acceptable and conservative.

If the average temperature of the flanges is the average of the inside temperature and the reactor pool water, assuming the 550 degrees Fahrenheit design temperature inside and a maximum possible reactor pool temperature of 212 degrees Fahrenheit outside the average flange temperature yields 381 degrees Fahrenheit, and a stud temperature of 212 degrees Fahrenheit.

These thermal conditions cause the flange to expand more than the stud and increase the joint tightness. In the analysis, both the flange and stud temperatures are set to the 550 degrees Fahrenheit design temperature. This slightly increases joint tightness because of higher thermal expansion in the flange compared to the stud. Using the design temperature in the analysis evaluates a bounding condition that is conservative, by allowing the joint to pry open or separate sooner.

The application of the thermal condition at each load step is discussed in Section 3.5.8.

3.5.8 CNV Pressure Capacity - Load Steps

Four load steps are used in the CNV pressure capacity ANSYS® models to apply the loads discussed in Section 3.5. The application of load steps is summarized in Table 3-4.

Load step 3 corresponds to the initial condition at design pressure, defined in Reference 6.1.1, Section C.1.c as the linear elastic response caused by dead load and design pressure, at the design temperature.

The internal pressure is incrementally increased from 1,000 psi to {{ }}$^{2(a)(c),\ ECI}$ by a minimum of ten substeps and a maximum of 30 substeps. Results for the substeps are inspected for the failure criteria defined in Section 3.1. The pressure capacity and joint gap opening of the CNV is determined by linear interpolation between the substep between 1,000 psi and {{ }}$^{2(a)(c),\ ECI}$ to determine the exact internal pressure to satisfy the failure criteria.

The pressure at which initial yielding (away from discontinuities) of the steel shell (not including cladding) or other steel components (flange covers, fasteners) occurs is also determined by linear interpolation between the substeps between 1,000 psi and {{ }}$^{2(a)(c),\ ECI}$. Initial yielding is defined by the end of the elastic curve at the design temperature. This pressure at initial yielding is recorded, per Reference 6.1.1, Section C.1.c.

Table 3-4 Load steps – pressure, temperature and preload

Load Step	Time (s)	Pressure (psi)	Temperature (°F)(1)	Preload(2)
1	1	0	70	Load
2	2	0	70	Lock
3(3)	3	1,000	550	Lock
4(4)	4	{{ }}2(a)(c), ECI	550	Lock

Notes:

1. Temperature is applied as a thermal condition per the methodology in Section 3.5.7.
2. Preloads for the studs in all bolted openings are applied using bolt pretension in ANSYS® Mechanical™.
3. Initial condition (design pressure and design temperature of the CNV).
4. The actual pressure at CNV failure is interpolated between the substeps between load steps 3 and 4.

3.6 CNV Head Buckling Analysis

Under internal pressure, a potential failure mode of torispherical steel heads is postulated from buckling as a result of a hoop compression zone in the knuckle region (Reference 6.1.1). Both of the NuScale upper and lower CNV heads are torispherical.

A linear (eigenvalue) buckling analysis, including full static structural models, is performed for both CNV heads. Buckling does not occur if the first ten buckling mode shapes for a linear (eigenvalue) buckling analysis are negative. Positive load multipliers correspond to internal pressure in this analysis. The first buckling mode shape always yields the lowest load multiplier. Therefore, additional buckling mode shapes generate higher load multipliers. If the first ten mode shapes yield load multipliers that are negative, it is highly unlikely that additional mode shapes yield positive load multipliers.

For both the top and bottom head linear buckling analyses, the following steps are performed:

1. A linear static structural analysis is run to define a base internal pressure loading condition.

2. The eigenvalue analysis determines the load multipliers (eigenvalues) that scale the base loading condition for each buckling mode. The eigenvalues are negative or positive with the minimum buckling load calculated as the smallest absolute eigenvalue multiplied by the load. In this analysis, positive eigenvalues correspond to internal pressure. The smallest positive eigenvalue corresponds to the minimum internal pressure to cause buckling. If no positive eigenvalues are identified, buckling is not predicted for internal pressure

3.6.1 Containment Vessel Top Head Buckling Model - Boundary Conditions and Load Steps

For the CNV top head buckling model, a horizontal slice plane through the CNV shell is vertically located 2.5√(Rt) from the bottom of the knuckle region in the top head, where "R" is the inside radius of the CNV and "t" is the wall thickness at the location of the end of the knuckle region.

The model is constrained by applying an ANSYS® Workbench remote displacement that is distributed to the nodes on the bottom horizontal slice plane. The remote displacement is set to zero for the X, Y and Z translational and rotational degrees of freedom

An internal pressure of 100 psi (base loading condition) is applied to the internal surfaces in one load step. Endcap forces for the covers, proportional to the internal pressure, are applied at the cover bolt circle lines (acting outward, perpendicular to the flange face) of the CNV top head manway (CNV24) and CRDM access (CNV25) covers. Endcap force is calculated for each bolted flange as follows:

$$F_{endcap} = \frac{\pi(D_c^2)(P_{internal})}{4}$$ Equation 3-4

Where:

D_c = the flange cover outer sealing diameter and

$P_{internal}$ = the internal pressure of the CNV.

The metal temperature in the model is set to a uniform temperature of 550 degrees Fahrenheit.

The ANSYS® CNV head buckling models and boundary conditions for the CNV top head are shown in Figure 3-10.

{{

}}2(a),(c),ECI

Figure 3-10 CNV top head buckling model – boundary conditions and loads

3.6.2 Containment Vessel Bottom Head Buckling Model - Boundary Conditions and Load Steps

For the CNV bottom head buckling model, a horizontal slice plane through the CNV shell is vertically located 2.5√(Rt) from the top of the knuckle region in the bottom head, where "R" is the inside radius of the CNV and "t" is the wall thickness at the location of the end of the knuckle region.

A frictionless support is applied to the bottom of the CNV support skirt. The frictionless support constrains the displacement normal to the plane and allows the plane to freely move in the transverse direction. This support prevents rigid body motion in the vertical

(parallel to the Y-axis) direction. No additional vertical support is applied to allow the model to grow vertically (parallel to the Y-axis).

The model is constrained in the transverse direction by applying an ANSYS® Workbench™ remote displacement. The remote displacement is distributed to the nodes on the top slice plane. The remote displacement in the transverse X and Z directions and rotational X, Y and Z directions are set to zero. The vertical Y component is free to allow the model to grow vertically. The nodes on the top slice plane are coupled through a commands object.

The internal pressure is applied to the internal surfaces in one load step at 100 psi (base loading condition). An endcap pressure (calculated per Equation 3-1 where D_c equals the ID of the CNV vessel shell), proportional to the internal pressure, is applied to the top slice plane. The metal temperature in the model is set to a uniform temperature of 550 degrees Fahrenheit.

The ANSYS® CNV head buckling models and boundary conditions for the CNV bottom head are shown in Figure 3-11.

{{

}}2(a),(c),ECI

Figure 3-11 Containment Vessel bottom head buckling model - boundary conditions and loads

3.7 Meshing

The CNV pressure capacity models and CNV head buckling models are meshed using higher order SOLID186 3-D, 20-node structural solid elements, and SOLID187 3-D, 10-node tetrahedral solid elements, both exhibiting quadratic behavior. Both element types support plasticity, large displacement, and large strain capabilities. A minimum of three elements are used through the thickness of the CNV shell, not including elements through the cladding. The mesh is refined in the vicinity of the bolted openings, in order to accurately capture the strain behavior. The mesh was generated to minimize the number of tetrahedral elements and maximize the number of brick elements. The finite element mesh of the CNV pressure capacity models are shown in Figure 3-12 through Figure 3-14 for the CNV top section model, Figure 3-15 through Figure 3-18 for the CNV middle section model, and Figure 3-19 through Figure 3-21 for the CNV bottom section model. The finite element mesh for the CNV head buckling models is shown in Figure 3-22 through Figure 3-23 for the CNV top head buckling model and Figure 3-24 for the CNV bottom head buckling model.

{{

}}2(a),(c),ECI

Figure 3-12 Containment Vessel top section model – mesh view on outside surface

{{

}}2(a),(c),ECI

Figure 3-13 Containment Vessel top section model – mesh view through thickness

{{

}}2(a),(c),ECI

Figure 3-14 Containment Vessel top section model – mesh view of control rod drive mechanism access (CNV25) and control rod drive mechanism electrical CNV37 closures

{{

}}2(a),(c),ECI

Figure 3-15 Containment Vessel middle section model – mesh view on outside surface

{{

}}2(a),(c),ECI

Figure 3-16 Containment Vessel middle section model – mesh view on inside surface

{{

}}2(a),(c),ECI

Figure 3-17 Containment Vessel middle section model – mesh view of steam generator inspection port closure (CNV30)

{{

}}2(a),(c),ECI

Figure 3-18 Containment Vessel middle section model – mesh view of the pressurizer access closure (CNV31)

{{

}}2(a),(c),ECI

Figure 3-19 Containment Vessel bottom section model – mesh view of refueling region

{{

}}2(a),(c),ECI

Figure 3-20 Containment Vessel bottom section model – mesh view of bottom head region

{{

}}2(a),(c),ECI

Figure 3-21 Containment Vessel bottom section model – mesh plane view through refueling region

{{

}}2(a),(c),ECI

Figure 3-22 Containment Vessel top head buckling model – mesh view outside

{{

}}2(a),(c),ECI

Figure 3-23 Containment Vessel top head buckling model – mesh view inside

{{

}}2(a),(c),ECI

Figure 3-24 Containment Vessel bottom head buckling model – mesh view

3.8 Software Use and Qualification

Per Reference 6.1.1, Section C.1.k.7, a description of the software used is to be provided. Three software programs are used in this report: ANSYS® Mechanical™ Version 16.0, operating within the ANSYS® Workbench™ 2.0 Framework; Microsoft® Excel 2010; and Parametric Technology Corporation Mathcad®.

ANSYS® Version 16.0 is pre-verified for use when used in the configuration controlled environment. Excel and Mathcad are not controlled and pre-verified for use, but results from the software are independently verified to assure that correct results are obtained. The analysis computer files used for this report are stored on NuScale's document record management program.

ANSYS® Version 16.0 is pre-verified for use in accordance with NuScale procedures and is configuration controlled. The NuScale computing environment used for the ANSYS® work in this calculation is shown in Table 3-5. The installation verification of ANSYS® Version 16.0 on the NuScale computing environment is performed to NuScale procedures.

Outstanding errors reported against ANSYS® were reviewed and no errors that would affect this calculation were found. The only warnings produced during execution are minor and related to material thermal expansion coefficients and reference temperature. These warnings do not affect the final results.

Excel and Mathcad were not pre-verified for use. Correct program input, application, and function are verified by a line-by-line review of equations and comparison to results obtained using a hand-held calculator. The computing environments used for the Excel and Mathcad work in this calculation are shown in Table 3-6 and Table 3-7.

Table 3-5 ANSYS® Computing Environment Information

Name	Description
Version	16.0
Operating system	Red Hat Enterprise Linux 6.4
System type	64-bit
Processor	Intel(R) Xeon(R) CPU E5-2690 v2 @ 3.00GHz (20 cores)

Table 3-6 Unverified computing environment information supporting analysis

Name	Description
Excel Version	14.0.7153.5000
Operating system	Windows 7 Professional
System type	64-bit
Processor	Intel® Core™ i7-5500U CPU @ 2.30 GHz

Table 3-7 Unverified computing environment information support revision

Name	Description
Excel Version	14.0.7153.5000
Mathcad Version	15.0
Operating system	Windows 7 Professional
System type	64-bit
Processor	Intel® Core™ i7-5500U CPU @ 2.40 GHz

4.0 Results

The results and conclusions of this calculation are presented in this section. The results are based on the methodology and calculations discussed in Section 3.0.

4.1 Initial Yielding

Per Reference 6.1.1, Section C.1.c the pressure to cause initial yielding is recorded. Minor plastic strain is first seen in the flange covers during the application of preload (load step 1 in Table 3-4). This strain subsequently increases at load step 3 (application of pressure and temperature). However, since this strain is small and not caused by the internal pressure, it is not considered for the determination of initial yielding.

Initial yielding as a result of internal pressure first occurs in the PZR Heater Access Port Covers (CNV31-32) at a pressure of approximately {{ }}$^{2(a)(c),\ ECI}$. The amount of plastic strain is small at this point.

Initial yielding of the CNV vessel shell (not including cladding), away from discontinuities, occurs in the CNV bottom section model in the CNV core region shell, below the lower transition shell at a pressure of approximately {{ }}$^{2(a)(c),\ ECI}$.

4.2 CNV Pressure Capacity and Flange Gaps

The red line shown in Figure 4-1 shows the region of surface contact for the PZR heater access (CNV31) bolted opening where the gap opening at the O-rings is evaluated. At a pressure of 1,240 psi, a flange gap of 0.03 inches begins to form at the outer O-ring. The color contours illustrated in Figure 4-2 show the gap opening of the region, as indicated by the red line in Figure 4-1. Negative values in Figure 4-2 indicate the gap size on the surface. The {{ }}$^{2(a)(c),\ ECI}$ minimum values (i.e., maximum gaps) shown in Figure 4-2 occur at a diameter smaller than the inner O-ring. The 0.03-inch gap opening at the outer O-ring meets CNV failure criterion A, defined in Section 3.1.

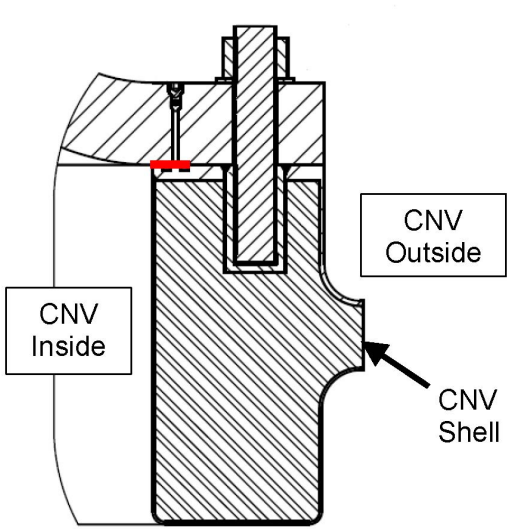

Figure 4-1 Pressurizer heater access (CNV31) flange and cover bolted opening.

{{

}}2(a)(c), ECI

Figure 4-2 Pressurizer heater access (CNV31) bolted opening flange gap at 1,240 psi.

The 0.03-inch gap opening at the inside of the PZR heater access port joint is a result of prying from the cover/flange. The prying is caused by the center of the cover expanding outward while being restrained at the edges by the studs. Figure 4-3 shows the prying that occurs on the joint and how a gap opens at the ID of the nozzle, but surface to surface contact remains at the OD. The 0.03-inch opening at the outer O-ring is the start of the joint failure. If pressure continues to increase more prying occurs and pressure is then able to progress out the flange under the cover. This creates more surface area for the pressure to act upon. The increased exposed area then creates more load to separate the joint and increases stress on the nut and stud. The 0.03-inch gap is an estimated opening that causes the pressure retaining seal to be lost. Any resulting reactor coolant system mass loss is minor because the outer edge of the joint remains in contact. The PZR heater access cover (CNV31) shown in Figure 4-2 is the most limiting failure location, and the largest opening occurs at the top and bottom edges of the cover. As the prying continues, the nut, stud, or threads fail at either the top or bottom of the cover where the prying is greatest. Once the first fastener fails the remaining fasteners are subject to an increased load. The remaining fasteners in turn quickly fail. This causes a cascading effect and the cover is lost. Prior to the loss of the first fastener there is only a minor loss of mass. Once the first fastener fails, there is a larger opening and pressure starts to decrease. However, the sequential failure of the other fasteners could occur quickly and the cover lost before any significant pressure loss occurs. This mode of failure is similar to the failures for metal containments discussed in Reference 6.1.2.

The discussion above describes a failure mode that is typical for vessels pressurized by single-phase gas, or two-phase liquid gas mixtures with significant stored energy as a result of the compressibility of the medium. The stored energy continues to exert stresses on the joint even after the failure of the first bolt, leading to the sequential failures. During a design basis accident, the inside of the CNV is a two-phase liquid gas mixture with liquid covering only the refueling flange inside of the CNV. The CNV does not become fully liquid solid.

The geometry of the bolted connection and flange gap at the seal surface for the CNV bolted openings evaluated in the CNV pressure capacity models is shown in Figure 4-4 through Figure 4-13. The gap openings on these bolted connection are shown at the 1,240 psi pressure causing a 0.030-inch gap for the PZR heater bolted connection. The contours on the contact surface show that the gaps on the remaining bolted connections remain closed or below the 0.03-inch gap at 1,240 psi.

{{

}}2(a)(c), ECI

Figure 4-3 Prying of pressurizer heater access (CNV31) bolted opening due to internal pressure

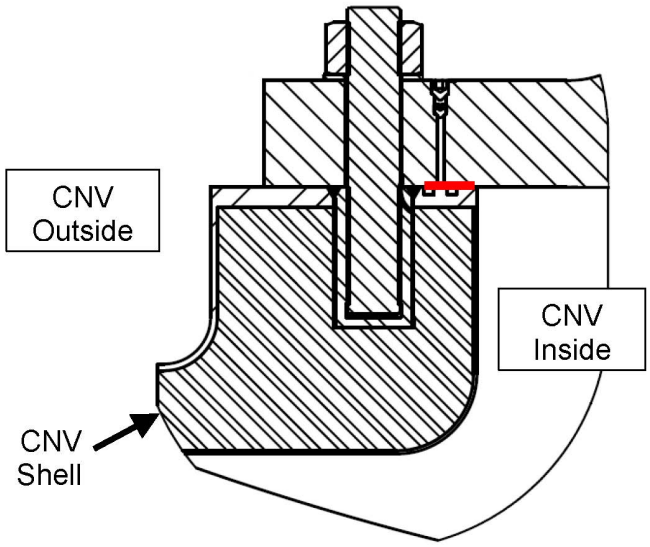

Figure 4-4 Steam generator inspection (CNV30) flange and cover bolted opening

{{

}}2(a)(c), ECI

Figure 4-5 Steam generator inspection (CNV30) bolted opening flange gap at 1,240 psi

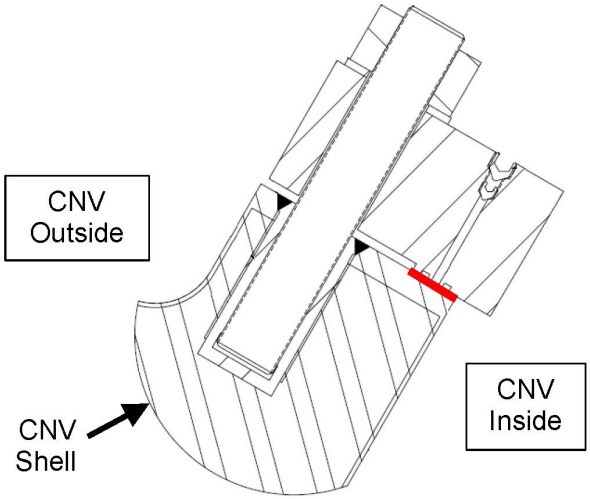

Figure 4-6 Containment Vessel top head manway (CNV24) flange and cover bolted opening

{{

}}2(a)(c), ECI

Figure 4-7 Containment Vessel top head manway (CNV24) bolted opening flange gap at 1,240 psi

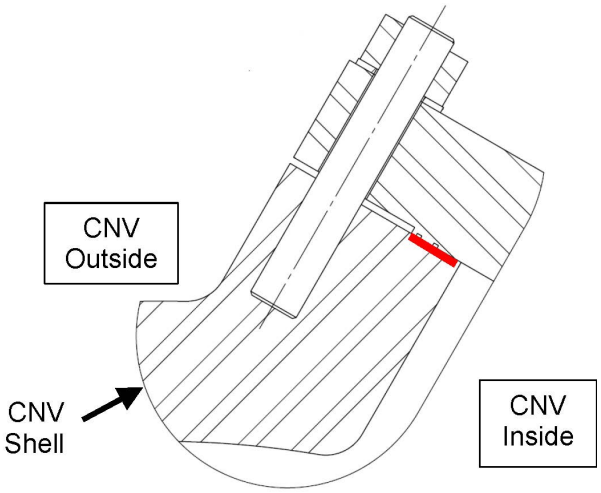

Figure 4-8 Control rod drive mechanism power (CNV37) flange and cover bolted opening

{{

}}2(a)(c), ECI

Figure 4-9 Control rod drive mechanism power (CNV37) bolted opening flange gap at 1,240 psi

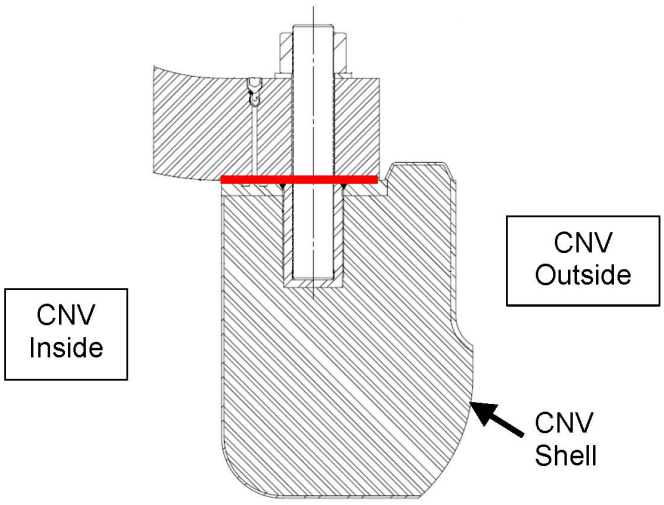

Figure 4-10 Control rod drive mechanism access (CNV25) flange and cover bolted opening

{{

}}2(a)(c), ECI

Figure 4-11 Control rod drive mechanism access (CNV25) bolted opening flange gap at 1,240 psi

{{

}}2(a)(c), ECI

Figure 4-12 Containment Vessel refueling closure flange bolted opening

{{

}}2(a)(c), ECI

Figure 4-13 Containment Vessel refueling closure flanges – inner flange gap at 1,240 psi

The contoured gap openings shown in Figure 4-2 through Figure 4-13 illustrate that the flange gaps at the outer O-rings are below the failure criterion of 0.03 in. In Figure 4-2 and Figure 4-5, the gap formed at the O-rings is not uniform; it is higher at locations along the vertical (Y) axis. This uneven gap is caused by increased radial deformation of the vessel wall between the SG inspection port (CNV30) and the PZR heater access port (CNV31) relative to the vessel deformation away from the bolted openings. The effective radius of the CNV in the vicinity of these large-diameter flanges is greater than the radius of the CNV away from the flanges, resulting in greater hoop strain in the vicinity of the large-diameter flanges. A small difference in the flange gap between locations along the horizontal (X and Z) axes is also seen in Figure 4-11 for the CRDM access opening (CNV25).

The flange gaps shown in the figures above are determined by manually selecting points along the outer O-rings using the probe tool in ANSYS® Mechanical™. The ratio of the gap at the CNV ultimate pressure capacity, determined using the manually selected points to the minimum flange gap (at the inner sealing diameter), is used to calculate the flange gaps at the outer O-rings for the CRDM access opening (CNV25), SG inspection port (CNV30), and PZR heater access port (CNV31), for pressures from 1,000 psi (load step 3) to {{ }}$^{2(a)(c),\ ECI}$ (load step 4)[3]. These flange gaps are shown in Table 4-1 and plotted in Figure 4-14. Due to the uneven deformation, two flange gap values (90 degrees apart) are provided at each pressure value, for each bolted opening.

Table 4-1 Flange Gap vs. Pressure from 1,000 psi to {{ }}$^{2(a)(c),\ ECI}$

Internal Pressure (psi)	Flange Gap at Outer O-ring (in)					
	CNV25 (CRDM)		CNV30 (SG)		CNV31 (PZR)	
	X-axis	Z-axis	Vertical	Horizontal	Vertical	Horizontal
1,000	2.54E-03	3.56E-03	3.97E-03	1.86E-03	1.70E-02	7.55E-03
{{ }}$^{2(a)(c),\ ECI}$	2.76E-03	3.87E-03	4.35E-03	2.04E-03	1.89E-02	8.41E-03
{{ }}$^{2(a)(c),\ ECI}$	3.03E-03	4.24E-03	4.78E-03	2.24E-03	2.13E-02	9.46E-03
{{ }}$^{2(a)(c),\ ECI}$	3.32E-03	4.65E-03	5.27E-03	2.47E-03	2.40E-02	1.07E-02
{{ }}$^{2(a)(c),\ ECI}$	3.66E-03	5.12E-03	5.83E-03	2.73E-03	2.72E-02	1.21E-02
{{ }}$^{2(a)(c),\ ECI}$	4.03E-03	5.64E-03	6.46E-03	3.03E-03	3.10E-02	1.38E-02
{{ }}$^{2(a)(c),\ ECI}$	4.45E-03	6.23E-03	7.23E-03	3.38E-03	3.56E-02	1.58E-02
{{ }}$^{2(a)(c),\ ECI}$	4.96E-03	6.94E-03	8.15E-03	3.82E-03	4.13E-02	1.83E-02
{{ }}$^{2(a)(c),\ ECI}$	5.58E-03	7.81E-03	9.30E-03	4.36E-03	4.90E-02	2.18E-02
{{ }}$^{2(a)(c),\ ECI}$	6.36E-03	8.91E-03	1.10E-02	5.13E-03	5.89E-02	2.62E-02
{{ }}$^{2(a)(c),\ ECI}$	7.31E-03	1.02E-02	1.34E-02	6.28E-03	7.22E-02	3.21E-02

[3] The other bolted openings are not included since the gap at the outer O-ring remains below 0.03 inch for pressures up to {{ }}$^{2(a)(c),\ ECI}$ (load step 4).

Internal Pressure (psi)	Flange Gap at Outer O-ring (in)					
	CNV25 (CRDM)		CNV30 (SG)		CNV31 (PZR)	
	X-axis	Z-axis	Vertical	Horizontal	Vertical	Horizontal
{{ }}[2(a)(c), ECI]	8.55E-03	1.20E-02	1.71E-02	8.02E-03	9.07E-02	4.03E-02
{{ }}[2(a)(c), ECI]	1.04E-02	1.45E-02	2.29E-02	1.07E-02	1.17E-01	5.22E-02
{{ }}[2(a)(c), ECI]	1.27E-02	1.78E-02	3.16E-02	1.48E-02	1.56E-01	6.92E-02
{{ }}[2(a)(c), ECI]	1.65E-02	2.32E-02	4.56E-02	2.14E-02	2.14E-01	9.52E-02
{{ }}[2(a)(c), ECI]	2.20E-02	3.07E-02	6.58E-02	3.08E-02	2.97E-01	1.32E-01
{{ }}[2(a)(c), ECI]	3.11E-02	4.35E-02	9.27E-02	4.34E-02	4.05E-01	1.80E-01

{{

}}[2(a)(c), ECI]

Figure 4-14 Flange gaps versus pressure from 1,000 psi to {{ }}[2(a)(c), ECI]

As shown in Figure 4-14, the PZR heater access port (CNV31) flange gap reaches 0.03 inch (along the vertical plane) at approximately 1,240 psi. CRDM access opening (CNV25) and SG inspection port (CNV30) first reach a flange gap of 0.03 inch at approximately {{ }}[2(a)(c), ECI] and {{ }}[2(a)(c), ECI], respectively.

The gap contours shown in Figure 4-7 and Figure 4-9 show that a small gap opens for these NPS 18 covers and are smaller than the other covers. The openings smaller than NPS 18 have bolting configurations similar to these covers. This reinforces the modeling assumption that not including the smaller openings is valid.

4.3 Loss of Stud Preload

The stud preload calculated using the methodology in Section 3.5.6 is shown in Table 4-2. Appendix C shows the calculations for the preload and the pressure needed to cause loss of preload (joint tightness) for each joint using this preload. The calculated pressure value needed to cause loss of preload is shown in Table 4-2. The pressures are above the 1,240 psi pressure needed to open the gap at the outer O-ring for the PZR heater access port. The {{ }}$^{2(a)(c), ECI}$ is the lowest pressure to lose bolt preload at 2,200 psi. Other pressures to lose bolt preload are more than double the pressure to open a 0.03 gap at an outer O-ring. Therefore, Criteria B in Section 3.1 is satisfied that the bolt preload is not lost.

Table 4-2 Stud Preload and Pressure to Lose Preload

Access Opening	Preload (lbf)	Pressure to Lose Preload (psi)
Refueling closure flange	{{ }}$^{2(a)(c), ECI}$	{{ }}$^{2(a)(c), ECI}$
Manway (head), CNV24	{{ }}$^{2(a)(c), ECI}$	{{ }}$^{2(a)(c), ECI}$
CRDM access, CNV25	{{ }}$^{2(a)(c), ECI}$	{{ }}$^{2(a)(c), ECI}$
SG inspection, CNV27-30	{{ }}$^{2(a)(c), ECI}$	{{ }}$^{2(a)(c), ECI}$
PZR access, CNV31-32	{{ }}$^{2(a)(c), ECI}$	{{ }}$^{2(a)(c), ECI}$
CRDM power, CNV37	{{ }}$^{2(a)(c), ECI}$	{{ }}$^{2(a)(c), ECI}$

4.4 Evaluation of Hoop Strain

As discussed in Section 4.1, initial yielding of the CNV vessel shell (not including cladding), away from discontinuities, occurs in the CNV bottom section model in the CNV core region shell. The maximum total (elastic + plastic) hoop strain is evaluated at this location as well as four other paths along the CNV. Table 4-3 shows the maximum total hoop strain at these locations for pressures from 1,000 psi (load step 3) to {{ }}$^{2(a)(c), ECI}$ (load step 4).

Table 4-3 Maximum total hoop strain from 1,000 psi to {{ }}2(a)(c), ECI

Internal Pressure (psi)	Maximum Total Hoop Strain (%) Global Vertical (Y axis) Path Location (inches)(1)				
	{{ }}2(a)(c), ECI	{{ }}2(a)(c), ECI	{{ }}2(a)(c), ECI	{{ }}2(a)(c), ECI	{{ }}2(a)(c), ECI
1,000	0.1%	0.1%	0.1%	0.1%	0.1%
{{ }}2(a)(c), ECI	0.1%	0.1%	0.1%	0.1%	0.1%
{{ }}2(a)(c), ECI	0.1%	0.1%	0.1%	0.1%	0.1%
{{ }}2(a)(c), ECI	0.1%	0.1%	0.1%	0.1%	0.1%
{{ }}2(a)(c), ECI	0.1%	0.1%	0.1%	0.1%	0.1%
{{ }}2(a)(c), ECI	0.1%	0.1%	0.1%	0.1%	0.1%
{{ }}2(a)(c), ECI	0.1%	0.1%	0.1%	0.1%	0.1%
{{ }}2(a)(c), ECI	0.1%	0.1%	0.1%	0.1%	0.1%
{{ }}2(a)(c), ECI	0.1%	0.1%	0.1%	0.1%	0.1%
{{ }}2(a)(c), ECI	0.1%	0.1%	0.1%	0.1%	0.1%
{{ }}2(a)(c), ECI	0.1%	0.1%	0.1%	0.1%	0.2%
{{ }}2(a)(c), ECI	0.2%	0.1%	0.1%	0.2%	0.2%
{{ }}2(a)(c), ECI	0.2%	0.2%	0.2%	0.3%	0.2%
{{ }}2(a)(c), ECI	0.2%	0.3%	0.4%	0.4%	0.3%
{{ }}2(a)(c), ECI	0.2%	0.6%	0.9%	0.9%	0.3%
{{ }}2(a)(c), ECI	0.2%	1.1%	1.5%	1.4%	0.4%
{{ }}2(a)(c), ECI	0.2%	1.6%	2.1%	2.0%	0.5%

Notes:
1. The path locations listed above are referenced to NuScale Power Module global zero (see Section 3.4.2)
2. Above the CNV refueling flanges in the CNV upper flange shell
3. Below the CNV refueling flanges in the CNV lower flange shell
4. Midway between the CNV refueling flanges and the transition shell in the CNV lower flange shell
5. Above the transition shell in the CNV lower flange shell
6. Below the transition shell in the CNV core region shell

As shown in Table 4-3, a maximum total hoop strain of 1.5 percent is reached in the CNV shell, away from discontinuities, at a pressure of about 1,750 psi. This corresponds to failure Criterion C, as defined in Section 3.1. However, as discussed in Section 4.2, the pressure capacity of the CNV meets Criterion A at a pressure of approximately 1,240 psi.

The non-linear plastic solution of the CNV pressure capacity models converge up to the final load step at {{ }}$^{2(a)(c), ECI}$ and no solution divergence occurred.

4.5 Containment Vessel Head Buckling Pressure

The load multipliers (eigenvalues) calculated for the first ten buckling modes for both CNV head buckling models are shown in Table 4-4 below. Buckling does not occur if the first ten load multipliers (eigenvalues), based on the first ten buckling mode shapes for a linear (eigenvalue) buckling analysis, are negative. Since the load multipliers are negative, buckling does not occur for the top or bottom CNV heads, subjected to internal pressure.

Table 4-4 Linear buckling eigenvalues

{{

}}$^{2(a)(c), ECI}$

To confirm the eigenvalue linear buckling results, hand calculations were done using buckling equations for torispherical knuckles provided in Reference 6.1.9. The buckling hand calculation is shown in Appendix D and shows that the bottom knuckle does not buckle until a high internal pressure of 4,556 psi . The top head knuckle does not buckle

until an even higher pressure of {{ }}[2(a)(c), ECI] is reached. The equations provide a conservative internal pressure when buckling actually occurs. These values are significantly above the 1,240 psi pressure shown in Section 4.2 for a 0.03 inch gap opening at the outer O-ring. This confirms knuckle buckling is at a high pressure and not be the limiting design feature for the CNV ultimate pressure.

5.0 Summary and Conclusions

This report evaluates the CNV to determine an ultimate pressure capacity for a beyond design basis LOCA event. Multiple finite element models and analyses were used to evaluate the bolted connections, shell regions away from concentrations, and buckling of the knuckle regions in the heads.

The CNV ultimate pressure capacity is determined to be 1,240 psi as a result of the PZR heater access cover displacing 0.03 inches at the cover's outer O-ring. This ultimate pressure capacity is above the 1,000 psi design pressure of the CNV and is calculated based on conservative analyses. Much of the conservatism in the analyses lies in use of the design temperature for material properties and in the plastic behavior (plastic modulus) modeled for the materials.

6.0 References

6.1 Referenced Documents

6.1.1 U.S. Nuclear Regulatory Commission, “Containment Structural Evaluation for Internal Pressure Loadings above Design-Basis Pressure,” Regulatory Guide 1.216, Revision 0, August 2010.

6.1.2 U.S. Nuclear Regulatory Commission, “Containment Integrity Research at Sandia National Laboratories – An Overview,” NUREG/CR-6906, July 2006.

6.1.3 U.S. Nuclear Regulatory Commission, “Standard Review Plan for the Review of Safety Analysis Reports for Nuclear Power Plants: LWR Edition — Design of Structures, Components, Equipment, and Systems,” NUREG-0800, Chapter 3, Section 3.8.2, Revision 3, May 2010.

6.1.4 *U.S. Code of Federal Regulations*, “Quality Assurance Criteria for Nuclear Power Plants and Fuel Reprocessing Facilities,” Appendix B, Part 50, Chapter 1, Title 10, “Energy,” (10 CFR 50, Appendix B).

6.1.5 American Society of Mechanical Engineers, *Quality Assurance Program Requirements for Nuclear Facility Applications*, NQA-1-2008, NQA-1a-2009 Addenda.

6.1.6 American Society of Mechanical Engineers, *Boiler and Pressure Vessel Code*, 2013 Edition, no addenda, Section II, “Materials,” Part D, Properties (Customary), July 1, 2013.

6.1.7 American Society of Mechanical Engineers, *Boiler and Pressure Vessel Code*, 2013 Edition, no addenda, Section III, “Rules for Construction of Nuclear Facility Components,” Division 1 – Subsection NB, Class 1 Components, July 1, 2013.

6.1.8 American Society of Mechanical Engineers, *Boiler and Pressure Vessel Code*, 2013 Edition, no addenda, Section III, “Rules for Construction of Nuclear Facility Components,” Appendices, July 1, 2013.

6.1.9 American Society of Mechanical Engineers, *Boiler and Pressure Vessel Code*, 2013 Edition, no addenda, Section VIII, “Rules for Construction of Pressure Vessels,” Division 2, Alternative Rules, July 1, 2013

6.1.10 American Society of Mechanical Engineers, *Unified Inch Screw Threads (UN and UNR Thread Form)*, ASME B1.1-2003, September 30, 2004.

6.1.11 Jones, F.D., et. al., *Machinery’s Handbook*, 26th Edition, Industrial Press Inc., New York, New York, 2000.

Appendix A. Endcap Pressure Calculations

This appendix calculates the endcap pressure load to be applied to the access covers in the CNV head buckling models. The calculations follow the methodology discussed in Section 3.5.5. The inputs to Equation 3-1 to calculate the endcap pressure are shown in Table A-1 and the calculated endcap pressures are shown in Table A-2.

Table A-1 Inputs to calculate endcap pressure load

Variable	Value	Units	Description
D_i	{{ }}$^{2(a)(c), ECI}$	inch	ID of the main CNV shell (including cladding)
D_o	{{ }}$^{2(a)(c), ECI}$	inch	OD of the main CNV shell (including cladding)
D_{c_CNV24}	{{ }}$^{2(a)(c), ECI}$	inch	Flange cover outer sealing diameter of CNV24
D_{c_CNV25}	{{ }}$^{2(a)(c), ECI}$	inch	Flange cover outer sealing diameter of CNV25
$P_{internal\_buckle}$	100	psi	Internal pressure of the CNV (for buckling analysis of CNV heads)

Table A-2 Calculated endcap pressure load

Output	Value	Units	Description
P_{endcap_3}	{{ }}$^{2(a)(c), ECI}$	psi	Endcap pressure at load step 3 (applied to CNV top head buckling model)
P_{endcap_4}	{{ }}$^{2(a)(c), ECI}$	psi	Endcap pressure at load step 4 (applied to CNV top head buckling model)
P_{endcap_buckle}	{{ }}$^{2(a)(c), ECI}$	psi	Endcap pressure for CNV bottom head buckling model

Appendix B. True Stress – True Strain Curves

The plastic modulus of the material stress-strain curves used to generate the results in this report are calculated using the material yield strength at design temperature (550 degrees Fahrenheit) and the percent elongation of the material at failure at room temperature. Equations to produce a materials true stress – true strain curve based on the materials yield strength, ultimate strength and modulus of elasticity at temperature are provided in Reference 6.1.9, Section 3-D.3.

The plastic modulus curves used in the analyses are compared to the calculated true stress – true strain curve. Figure B-1, Figure B-2, Figure B-3, Figure B-4, Figure B-5, Figure B-6 and Figure B-7 show the comparison for {{

}}$^{2(a)(c),\ ECI}$, respectively.

The comparison in the figures show that the plastic modulus used in the analyses have a lower slope than the true stress – true strain curves based on ASME Code properties at design temperature (550 degrees Fahrenheit). The reduced slope of the plastic modulus produces a pressure below where the CNV is expected to fail and therefore a conservative analysis.

A sample calculation using the equations from Reference 6.1.9, Section 3-D.3 is shown for one true stress – true strain point for SA-508 Grade 3, Class 2 material. For each material a series of these calculations is done to produce the full curve.

Sample calculation of SA-508 Grade 3, Class 2 true stress – true strain point:

SA-508 Grade 3, Class 2 true stress – true strain				
Inputs:				
Variable	**Material Property**		**Value**	**Units**
σ_{ys}	Engineering yield strength		55,400	psi
σ_{uts}	Engineering ultimate tensile strength		90,000	psi
E_y	Modulus of elasticity		25,400,000	psi
Constant Calculations:				
Variable	**Eq. No**	**Constant Equations**	**Value**	**Units**
R	3-D.10	$\sigma_{ys} / \sigma_{uts}$	0.6155556	N/A
ε_{ys}	3-D.11		0.002	in/in
K	3-D.12	$1.5(R)^{1.5} - 0.5(R)^{2.5} - (R)^{3.5}$	0.3927886	----
m_2	Table 3-D.1	0.60(1.00 - R)	0.2306667	----
ε_p	Table 3-D.1		0.00002	in/in
A_2	3-D.8	$[(\sigma_{uts})\exp(m_2)] / (m_2)^{m_2}$	158985.65	----
m_1	3-D.6	$[\ln(R) + (\varepsilon_p - \varepsilon_{ys})] / \ln[\ln(1 + \varepsilon_p)/\ln(1 + \varepsilon_{ys})]$	0.1058191	----
A_1	3-D.5	$[\sigma_{ys}(1 + \varepsilon_{ys})] / [\ln(1 + \varepsilon_{ys})]^{m_1}$	107158.31	----
Calculations:				
Variable	**Eq. No.**	**Variable Constant Equations**	**Value**	**Units**
H	3-D.9	$\{ 2[\sigma_t - (\sigma_{ys} + K\{\sigma_{uts} - \sigma_{ys}\})] \} / [K(\sigma_{uts} - \sigma_{ys})]$	-2.000000	----
ε_2	3-D.7	$(\sigma_t / A_2)^{(1/m_2)}$	0.010354	in/in
ε_1	3-D.4	$(\sigma_t / A_1)^{(1/m_1)}$	0.001961	in/in
γ_2	3-D.3	$(\varepsilon_2 / 2)[1.0 + \tanh(H)]$	0.000186	in/in
γ_1	3-D.2	$(\varepsilon_1 / 2)[1.0 + \tanh(H)]$	0.000035	in/in
Results:				
Variable	**True Strain, True Stress**		**Value**	**Units**
ε_t	3-D.1	$(\sigma_t / E_y) + \gamma_1 + \gamma_2$	0.002403	in/in
σ_t	Input, true stress		55,400	psi

{{

}}2(a)(c), ECI

Figure B-1 True stress – true strain curve for SA-508 Grade 3, Class 2 at 550 degrees Fahrenheit

{{

}}2(a)(c), ECI

Figure B-2 True stress – true strain curve for SA-965 FXM19 at 550 degrees Fahrenheit

Technical Report

{{

}}2(a)(c), ECI

Figure B-3 True stress – true strain curve for SB-637 718 at 550 degrees Fahrenheit

{{

}}2(a)(c), ECI

Figure B-4 True stress – true strain curve for SA-564 Grade 630 at 550 degrees Fahrenheit

{{

}}2(a)(c), ECI

Figure B-5 True stress – true strain curve for SA-182 Type F304 at 550 degrees Fahrenheit

{{

}}2(a)(c), ECI

Figure B-6 True stress – true strain curve for SA-240 Type 304 at 550 degrees Fahrenheit

{{

}}2(a)(c), ECI

Figure B-7 True stress – true strain curve for SA-240 Type 304L at 550 degrees Fahrenheit

Appendix C. Tight Joint Evaluation

The equations to calculate the stud preload needed to maintain a tight joint are provided in Reference 6.1.8, Appendix E. These equations are solved to calculate a maximum internal pressure needed to obtain the maximum stud preload based on the stud material properties. Table C-1 shows the maximum internal pressure needed to maintain a tight joint with the maximum stud preload. Table C-2 shows the maximum stud preload based on the stud material properties, which is the stud preload applied in the analyses. The stud preload calculations follow the methodology discussed in Section 3.5.6.

Table C-1 Maximum pressure for maximum stud preload

Variable	Description	Equation/Source	Units	Closure	Top Head Manway (CNV24)	CRDM Access (CNV25)	SG Inspection (CNV27-30)	PZR Access (CNV31-32)	CRDM Power (CNV37)
w	O-ring width	Assumed	in	{{					}}$^{2(a)(c), ECI}$
m	Gasket factor	Ref. 6.1.8, Table E-1210-1	N/A	{{					}}$^{2(a)(c), ECI}$
b	Effective O-ring seating width	Ref. 6.1.8, Table E-1210-2	in	{{					}}$^{2(a)(c), ECI}$
P	Maximum Internal pressure	Input	psi	{{					}}$^{2(a)(c), ECI}$
G_i	Diameter of inside gasket	NuScale Drawing	in	{{					}}$^{2(a)(c), ECI}$
G_o	Diameter of outside gasket	NuScale Drawing	in	{{					}}$^{2(a)(c), ECI}$
n	Number studs	NuScale Drawing	N/A	{{					}}$^{2(a)(c), ECI}$
H_i	Total load to compress inside seal	$H_i = 2(b)(3.14)(G_i)(m)(p)$	lb	{{					}}$^{2(a)(c), ECI}$
H_o	Total load to compress outside seal	$Ho = 2(b)(3.14)(G_o)(m)(p)$	lb	{{					}}$^{2(a)(c), ECI}$
H	Total hydrostatic end force	$H = 0.785(G^2)(p)$	lb	{{					}}$^{2(a)(c), ECI}$
W_{m1}	Minimum required total stud load	$W_{m1} = H + H_i + H_o$	lb	{{					}}$^{2(a)(c), ECI}$
F_{Hi}	Load per stud to compress inside O-ring	H_i / n	lb	{{					}}$^{2(a)(c), ECI}$
F_{Ho}	Load per stud to compress outside O-ring	H_o / n	lb	{{					}}$^{2(a)(c), ECI}$
F_H	Load per stud for hydrostatic end force	H / n	lb	{{					}}$^{2(a)(c), ECI}$
F_{m1}	Required stud load	W_{m1} / n	lb	{{					}}$^{2(a)(c), ECI}$

Table C-2 Maximum stud preload

Variable	Description	Equation/Source	Units	Closure	Manway (Head) (CNV24)	CRDM Access (CNV25)	SG Inspection (CNV27-30)	PZR Access (CNV31-32)	CRDM Power (CNV37)
N/A	Stud size	NuScale Drawing	in	{{					}}$^{2(a)(c), ECI}$
n	Threads per inch	NuScale Drawing	1/in	{{					}}$^{2(a)(c), ECI}$
D_{p_min}	Minor pitch diameter	Ref. 6.1.10	in	{{					}}$^{2(a)(c), ECI}$
p	pitch	1 / n	in	{{					}}$^{2(a)(c), ECI}$
D_r	Minor thread diameter	D_{p_min} - 0.64951905(p)	in	{{					}}$^{2(a)(c), ECI}$
D_s	Shank diameter	NuScale Drawing	in	{{					}}$^{2(a)(c), ECI}$
A_{min}	Minimum area	$p(D_r^2)/4$	in^2	{{					}}$^{2(a)(c), ECI}$
N/A	Stud Material	NuScale Drawing	N/A	{{					}}$^{2(a)(c), ECI}$
S_m	Stud material yield stress	Table 2-2	psi	{{					}}$^{2(a)(c), ECI}$
F_i	Preload	$(2/3)S_y*A_{min}$	lb	{{					}}$^{2(a)(c), ECI}$
N/A	Check ratio of max. preload to preload required for max. pressure	F_i / F_{m1}	N/A	1.00	1.00	1.00	1.00	1.00	1.00

Appendix D. Head Knuckle Buckling Hand Calculation

Equations to predict buckling in a knuckle of a torispherical head due to internal pressure are provided in Reference 6.1.9, Section 4.3.6. The equations provide a conservative value of the internal pressure needed to cause buckling in a torispherical head knuckle. These calculations are used to confirm the eigenvalue linear buckling results. The actual values to produce buckling are expected to be larger than what these equations are calculating. Below are the calculations for the CNV bottom head and CNV top head. The equation numbers in this appendix refer to the equation numbers specified in Reference 6.1.9, Section 4.3.6.

Containment Vessel Bottom Head - Knuckle Buckling under Internal Pressure

Reference 6.1.9, Section 4.3.6.1, Torispherical Heads with the Same Crown and Knuckle Thicknesses.

Material properties of SA-965 FXM19 at design temperature

$E_T := 25.6 \cdot 10^6 psi$ Modulus of Elasticity at 550 degrees Fahrenheit (Reference 6.1.6, Table M-1).

$S_y := 38100 \cdot psi$ Yield strength at 550 degrees Fahrenheit (Reference 6.1.6, Table Y-1).

{{

}}2(a)(c), ECI

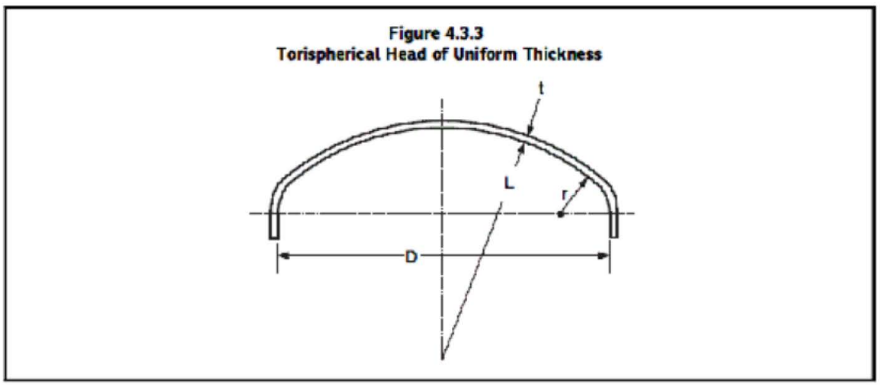

Figure D-1 Torispherical head geometry

Calculate geometry ratios:

$\frac{L}{D} = 0.901$ $\frac{r}{D} = 0.169$ $\frac{L}{t} = 38.583$

Where the following conditions are satisfied

$0.7 \le \frac{L}{D} \le 1.0$ $\frac{r}{D} \ge 0.06$ $20 \le \frac{L}{t} \le 2000$ Eq. 4.3.5, Eq. 4.3.6, Eq. 4.3.7

Calculate geometry constants:

$\beta_{th} := \operatorname{acos}\left(\frac{0.5 \cdot D - r}{L - r}\right) = 1.102$ radians Eq. 4.3.8

$\phi_{th} := \frac{\sqrt{L \cdot t}}{r} = 0.856$ radians Eq. 4.3.9

$$R_{th} := \begin{cases} \frac{0.5 \cdot D - r}{\cos\left(\beta_{th} - \phi_{th}\right)} + r & \text{if } \phi_{th} < \beta_{th} \\ 0.5 \cdot D & \text{otherwise} \end{cases}$$ Eq. 4.3.10 Eq. 4.3.11

$R_{th} = 65.562\,\text{in}$

Calculate coefficients:

$$C_1 := \begin{cases} 9.31 \cdot \left(\frac{r}{D}\right) - 0.086 & \text{if } \frac{r}{D} \le 0.08 \\ 0.692 \cdot \left(\frac{r}{D}\right) + 0.605 & \text{otherwise} \end{cases}$$ Eq. 4.3.12 Eq. 4.3.13

$C_1 = 0.722$

$$C_2 := \begin{cases} 1.25 & \text{if } \frac{r}{D} \le 0.08 \\ 1.46 - 2.6 \cdot \left(\frac{r}{D}\right) & \text{otherwise} \end{cases}$$ Eq. 4.3.14 Eq. 4.3.15

$C_2 = 1.02$

Calculate internal pressure expected to produce elastic buckling of the knuckle

$$P_{eth} := \frac{C_1 \cdot E_T \cdot t^2}{C_2 \cdot R_{th} \cdot \left(\frac{R_{th}}{2} - r \right)} = 225831\,psi \qquad \text{Eq. 4.3.16}$$

Since the allowable stress at 300 °F temperature is governed by time-independent properties, then

$C_3 := S_y = 38100\,psi$

Calculate internal pressure that will result in a maximum stress in the knuckle equal to the material yield strength

$$P_y := \frac{C_3 \cdot t}{C_2 \cdot R_{th} \cdot \left(\frac{R_{th}}{2 \cdot r} - 1 \right)} = 3376\,psi \qquad \text{Eq. 4.3.17}$$

Calculate internal pressure expected to result in a buckling failure of the knuckle

$$G := \frac{P_{eth}}{P_y} = 66.9 \qquad \text{Eq. 4.3.20}$$

$$P_{ck} := \begin{cases} 0.6 \cdot P_{eth} & \text{if } G \le 1 \\ \dfrac{0.77508 \cdot G - 0.20354 \cdot G^2 + 0.019274 \cdot G^3}{1 + 0.19014 \cdot G - 0.089534 \cdot G^2 + 0.0093965 \cdot G^3} \cdot P_y & \text{otherwise} \end{cases} \qquad \text{Eq. 4.3.18, Eq. 4.3.19}$$

$P_{ck} = 6833\,psi$

Allowable pressure based on buckling of the knuckle

$$P_{ak} := \frac{P_{ck}}{1.5} = 4556\,psi \qquad \text{Eq. 4.3.21}$$

Containment Vessel Top Head - Knuckle Buckling under Internal Pressure

Reference 6.1.9, Section 4.3.6.1, Torispherical Heads with the Same Crown and Knuckle Thicknesses.

Material properties of SA-508 Grade 3 Class 2 at design temperature

$E_T := 25.4 \cdot 10^6 psi$ Modulus of Elasticity at 550 °F (Reference 6.1.6, Table M-1)

$S_y := 55400 \cdot psi$ Yield strength at 550 °F. (Reference 6.1.6, Table Y-1, Page 628, Line 10)

{{

}}2(a)(c), ECI

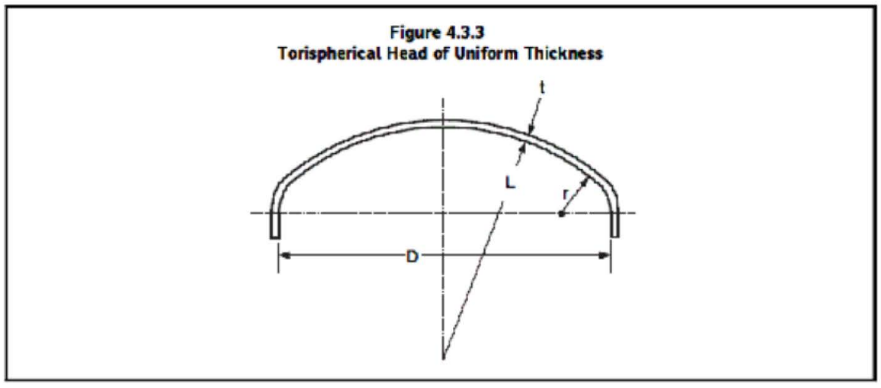

Figure D-2 Torispherical head geometry

Calculate geometry ratios:

$\frac{L}{D} = 0.8$ $\frac{r}{D} = 0.15$ $\frac{L}{t} = 27.24$

where the following conditions are satisfied

$0.7 \le \frac{L}{D} \le 1.0$ $\frac{r}{D} \ge 0.06$ $20 \le \frac{L}{t} \le 2000$ Eq. 4.3.5, Eq. 4.3.6, Eq. 4.3.7

Calculate geometry constants:

$$\beta_{th} := \operatorname{acos}\left(\frac{0.5\cdot D - r}{L - r}\right) = 1.002 \quad \text{radians} \qquad \text{Eq. 4.3.8}$$

$$\phi_{th} := \frac{\sqrt{L\cdot t}}{r} = 1.022 \quad \text{radians} \qquad \text{Eq. 4.3.9}$$

$$R_{th} := \begin{cases} \dfrac{0.5\cdot D - r}{\cos\left(\beta_{th} - \phi_{th}\right)} + r & \text{if } \phi_{th} < \beta_{th} \qquad \text{Eq. 4.3.10} \\ 0.5\cdot D & \text{otherwise} \qquad \text{Eq. 4.3.11} \end{cases}$$

$$R_{th} = 85.125\,\text{in}$$

Calculate coefficients:

$$C_1 := \begin{cases} 9.31\cdot\left(\dfrac{r}{D}\right) - 0.086 & \text{if } \dfrac{r}{D} \le 0.08 \qquad \text{Eq. 4.3.12} \\ 0.692\cdot\left(\dfrac{r}{D}\right) + 0.605 & \text{otherwise} \qquad \text{Eq. 4.3.13} \end{cases}$$

$$C_1 = 0.709$$

$$C_2 := \begin{cases} 1.25 & \text{if } \dfrac{r}{D} \le 0.08 \qquad \text{Eq. 4.3.14} \\ 1.46 - 2.6\cdot\left(\dfrac{r}{D}\right) & \text{otherwise} \qquad \text{Eq. 4.3.15} \end{cases}$$

$$C_2 = 1.07$$

Calculate internal pressure expected to produce elastic buckling of the knuckle

$$P_{eth} := \frac{C_1\cdot E_T\cdot t^2}{C_2\cdot R_{th}\cdot\left(\dfrac{R_{th}}{2} - r\right)} = 290260\,\text{psi} \qquad \text{Eq. 4.3.16}$$

Since the allowable stress at 300 °F temperature is governed by time-independent properties, then

$$C_3 := S_y = 55400\,\text{psi}$$

Calculate internal pressure that will result in a maximum stress in the knuckle equal to the material yield strength

$$P_y := \frac{C_3 \cdot t}{C_2 \cdot R_{th} \cdot \left(\frac{R_{th}}{2 \cdot r} - 1 \right)} = 4562\,\text{psi} \qquad \text{Eq. 4.3.17}$$

Calculate internal pressure expected to result in a buckling failure of the knuckle

$$G := \frac{P_{eth}}{P_y} = 63.626 \qquad \text{Eq. 4.3.20}$$

$$P_{ck} := \begin{cases} 0.6 \cdot P_{eth} & \text{if } G \le 1 \\ \dfrac{0.77508 \cdot G - 0.20354 \cdot G^2 + 0.019274 \cdot G^3}{1 + 0.19014 \cdot G - 0.089534 \cdot G^2 + 0.0093965 \cdot G^3} \cdot P_y & \text{otherwise} \end{cases} \qquad \text{Eq. 4.3.18} \quad \text{Eq. 4.3.19}$$

$$P_{ck} = 9230\,\text{psi}$$

Allowable pressure based on buckling of the knuckle

{{ }}$^{2(a)(c),\ ECI}$ Eq. 4.3.21

Enclosure 3:

Affidavit of Thomas a. Bergman, AF-1217-57526

NuScale Power, LLC
1100 NE Circle Blvd., Suite 200 Corvallis, Oregon 97330 Office 541.360-0500 Fax 541.207.3928
www.nuscalepower.com

NuScale Power, LLC

AFFIDAVIT of Thomas A. Bergman

I, Thomas A. Bergman, state as follows:

(1) I am the Vice President of Regulatory Affairs of NuScale Power, LLC (NuScale), and as such, I have been specifically delegated the function of reviewing the information described in this Affidavit that NuScale seeks to have withheld from public disclosure, and am authorized to apply for its withholding on behalf of NuScale.

(2) I am knowledgeable of the criteria and procedures used by NuScale in designating information as a trade secret, privileged, or as confidential commercial or financial information. This request to withhold information from public disclosure is driven by one or more of the following:

(a) The information requested to be withheld reveals distinguishing aspects of a process (or component, structure, tool, method, etc.) whose use by NuScale competitors, without a license from NuScale, would constitute a competitive economic disadvantage to NuScale.

(b) The information requested to be withheld consists of supporting data, including test data, relative to a process (or component, structure, tool, method, etc.), and the application of the data secures a competitive economic advantage, as described more fully in paragraph 3 of this Affidavit.

(c) Use by a competitor of the information requested to be withheld would reduce the competitor's expenditure of resources, or improve its competitive position, in the design, manufacture, shipment, installation, assurance of quality, or licensing of a similar product.

(d) The information requested to be withheld reveals cost or price information, production capabilities, budget levels, or commercial strategies of NuScale.

(e) The information requested to be withheld consists of patentable ideas.

(3) Public disclosure of the information sought to be withheld is likely to cause substantial harm to NuScale's competitive position and foreclose or reduce the availability of profit-making opportunities. The accompanying technical report reveals distinguishing aspects about the method by which NuScale develops its Containment Vessel Ultimate Pressure Integrity Technical Report.

NuScale has performed significant research and evaluation to develop a basis for this method and has invested significant resources, including the expenditure of a considerable sum of money.

The precise financial value of the information is difficult to quantify, but it is a key element of the design basis for a NuScale plant and, therefore, has substantial value to NuScale.

If the information were disclosed to the public, NuScale's competitors would have access to the information without purchasing the right to use it or having been required to undertake a similar expenditure of resources. Such disclosure would constitute a misappropriation of NuScale's intellectual property, and would deprive NuScale of the opportunity to exercise its competitive advantage to seek an adequate return on its investment.

(4) The information sought to be withheld is in the enclosed technical report entitled "Containment Vessel Ultimate Pressure Integrity." The enclosure contains the designation "Proprietary" at the top of each page containing proprietary information. The information considered by NuScale to be proprietary is identified within double braces, "{{ }}" in the document.

(5) The basis for proposing that the information be withheld is that NuScale treats the information as a trade secret, privileged, or as confidential commercial or financial information. NuScale relies upon the exemption from disclosure set forth in the Freedom of Information Act ("FOIA"), 5 USC § 552(b)(4), as well as exemptions applicable to the NRC under 10 CFR §§ 2.390(a)(4) and 9.17(a)(4).

(6) Pursuant to the provisions set forth in 10 CFR § 2.390(b)(4), the following is provided for consideration by the Commission in determining whether the information sought to be withheld from public disclosure should be withheld:

(a) The information sought to be withheld is owned and has been held in confidence by NuScale.

(b) The information is of a sort customarily held in confidence by NuScale and, to the best of my knowledge and belief, consistently has been held in confidence by NuScale. The procedure for approval of external release of such information typically requires review by the staff manager, project manager, chief technology officer or other equivalent authority, or the manager of the cognizant marketing function (or his delegate), for technical content, competitive effect, and determination of the accuracy of the proprietary designation. Disclosures outside NuScale are limited to regulatory bodies, customers and potential customers and their agents, suppliers, licensees, and others with a legitimate need for the information, and then only in accordance with appropriate regulatory provisions or contractual agreements to maintain confidentiality.

(c) The information is being transmitted to and received by the NRC in confidence.

(d) No public disclosure of the information has been made, and it is not available in public sources. All disclosures to third parties, including any required transmittals to NRC, have been made, or must be made, pursuant to regulatory provisions or contractual agreements that provide for maintenance of the information in confidence.

(e) Public disclosure of the information is likely to cause substantial harm to the competitive position of NuScale, taking into account the value of the information to NuScale, the amount of effort and money expended by NuScale in developing the information, and the difficulty others would have in acquiring or duplicating the information. The information sought to be withheld is part of NuScale's technology that provides NuScale with a competitive advantage over other firms in the industry. NuScale has invested significant human and financial capital in developing this technology and NuScale believes it would be difficult for others to duplicate the technology without access to the information sought to be withheld.

I declare under penalty of perjury that the foregoing is true and correct. Executed on December 14, 2017.

Thomas A. Bergman